energies

MDPI

Article

Modified Quasi-Opposition-Based Grey Wolf Optimization for Mathematical and Electrical Benchmark Problems

Salil Madhav Dubey [1], Hari Mohan Dubey [2] and Surender Reddy Salkuti [3,*]

[1] Department of Electrical Engineering, Madhav Institute of Technology & Science (MITS), Gwalior 474005, India
[2] Department of Electrical Engineering, Birsa Institute of Technology Sindri (BIT Sindri), Sindri, Dhanbad 828123, India
[3] Department of Railroad and Electrical Engineering, Woosong University, Daejeon 34606, Korea
* Correspondence: surender@wsu.ac.kr

Abstract: This paper proposes a modified quasi-opposition-based grey wolf optimization (mQOGWO) method to solve complex constrained optimization problems. The effectiveness of mQOGWO is examined on (i) 23 mathematical benchmark functions with different dimensions and (ii) four practical complex constrained electrical problems that include economic dispatch of 15, 40, and 140 power generating units and a microgrid problem with different energy sources. The obtained results are compared with the reported results using other methods available in the literature. Considering the solution quality of all test cases, the proposed technique seems to be a promising alternative for solving complex constrained optimization problems.

Keywords: quasi-opposed learning; grey wolf optimizer; mathematical benchmark; electrical benchmark; box plot analysis; microgrid

Citation: Dubey, S.M.; Dubey, H.M.; Salkuti, S.R. Modified Quasi-Opposition-Based Grey Wolf Optimization for Mathematical and Electrical Benchmark Problems. *Energies* **2022**, *15*, 5704. https://doi.org/10.3390/en15155704

Academic Editor: José Matas

Received: 13 June 2022
Accepted: 2 August 2022
Published: 5 August 2022

1. Introduction

Optimization is finding the best solution in terms of the highest performance under the given constrained or most cost-effective solution for a variable of a specific problem to maximize/minimize an objective function. The solution to practical optimization problems is very difficult as it is restricted by the lack of complete information and time to evaluate it. Researchers have applied various traditional optimization methods (TOM) such as non-linear programming (NLP), dynamic programming (DP), and geometrical programming (GP) for the solution of practical constrained optimization problems. Although traditional optimization methods have performed well for various practical cases, they have some limitations related to their search mechanism. The strategy related to the search mechanism generally depends on the objective function and associated constraints. The solution of the objective function also depends on the dimension of the problem, the nature of the objective function (convex or non-convex), and the initial solution of the selected problem. TOM does not provide a simple solution approach that can be utilized for the solution of a problem where different types of variables, objective functions, and related constraints are used. Real-world optimization problems have multiple variables and complex operational constraints that influence the modeling, making objective function non-linear, multimodal and discontinuous. These types of problems cannot be solved efficiently by TOM. Researchers have been conducting studies in this field, and nature-inspired optimization (NIO) has been suggested as an alternative to deal with such practical complexity. These non-traditional methods (metaheuristics) can guarantee faster convergence than TOM but may not always guarantee a global optimum. Therefore, various advanced optimization methods came into existence and became popular in recent decades [1]. All metaheuristics utilize some or other kind of randomization to find a set of solutions, and it has two common phases: exploration and exploitation. A metaheuristic will be successful on a given optimization

problem if it can provide a proper balance between exploration and exploitation [2]. The main criteria to differentiate one metaheuristic from the other is how an algorithm achieves this balance. The existing metaheuristic may be grouped into broad categories as evolutionary algorithms (EA) [3,4], swarm intelligence-based algorithms (SIA) [5–13], ecology-based algorithms (ECOA) [14–16], and physical science-based algorithms (PSA) [17–21].

EAs utilize the concept of biological evolution as reproduction, mutation, recombination, and selection. The genetic algorithm [3] and the differential evolution [4] are EAs. SIAs utilize the concept of self-organized and group behavior during the optimization process. Popular examples of SIAs are ant colony optimization (ACO) [5], which is based on the process of ants seeking the shortest path between colony and food source; particle swarm optimization (PSO) [6,7], inspired by the social behavior of fish schooling or bird flocking; artificial bee colony (ABC) optimization [8], inspired by the intelligent foraging behavior of honey bee swarm; the firefly algorithm (FFA) [9], inspired by the flashing behavior of fireflies; the krill herd algorithm (KHA) [10] simulates the heading behavior of krill; the bacterial foraging algorithm (BFA) [11], inspired by the social foraging behavior of E Coli bacteria; whale optimization (WO) [12] simulates the bubble-net hunting mechanism of humpback whales; grey wolf optimization (GWO) [13] simulates the leadership and social hierarchy of grey wolf when hunting prey.

The concept of migration of species between habitats is utilized in biogeography-based optimization [14], the idea of a variable rate of pulse emission and loudness is used in the bat algorithm [15], and the flower pollination algorithm mimics the pollination process of flowers [16]. All of these are examples of ECOAs [14–16].

The physical process of heating and slowly lowering the temperature to minimize material defects is utilized in modeling of the simulated annealing (SA) algorithm [17]. The gravitation search algorithm (GSA) uses the Newtonian law of gravity [18]. teacher learner-based optimization (TLBO) [19,20] simulates the teaching and learning phenomenon in a classroom. The chemical reaction optimization (CRO) [21] simulates the process of transforming the molecules through a sequence of reactions into a product. All of these are examples of PSAs.

Grey wolf optimization (GWO) is a SIA that was proposed by Mirjalili et al. in 2014 [13]. Its analytical model imitates the collective behavior in a group of individuals and the leadership hierarchy of grey wolves for hunting prey. Numerous variants of GWO have been proposed to solve complex constrained practical optimization problems. GWO and its variants have been successfully applied to solve several real-world optimization problems related to science and technology [22]. These are summarized in Table 1 below.

Table 1. Variants of GWO over the years along with the domain of application.

Method	Modification	Domain of Application
GWO	N.A.	Mathematical benchmark, welded beam design, pressure vessel design, optical buffer design [13], economic dispatch (ED) [23], short-term hydro-thermal scheduling (STHTS) [24], combined heat and power (CHP) with ED [25], microgrids [26], distribution generator (DG) placement [27], controller design [28–30], wireless networks [31,32], image processing [33,34], regular design [35], and parameter estimation [36].
Complex-Valued Encoding Grey Wolf Optimizer (CGWO)	DE/best/2 mutation strategy is embedded with GWO.	Mathematical benchmark and infinite impulse response (IIR) model identification [37].
Powell Local Optimization-Based Grey Wolf Optimizer (PGWO)	Powell method is embedded with GWO.	Mathematical benchmark and Data Clustering [38].

Table 1. *Cont.*

Method	Modification	Domain of Application
Hybrid Grey Wolf Optimizer (HGWO)	DE/best/1 and dynamic crossover rate are implanted in GWO.	ED [39].
Modified Grey Wolf Optimizer (mGWO)	Exponential decay of 'a' is utilized here in place of linear decay.	Mathematical benchmark and cluster head selection problem in Wireless Sensor Networks (WSNs) [40].
Chaos-Based Grey Wolf Optimizer (Ch-GWO)	Tent and Singer map is used to enhance global search capability.	Position control of a robotic manipulator [41].
Mean Grey Wolf Optimizer (MGWO)	Encircling the pray phase of GWO is carried out by considering the mean distance of grey wolves from the prey.	Mathematical benchmark and real-life dataset problems [42].
Ameliorated Grey Wolf Optimizer (Am-GWO)	Exploratory search mechanism to ensure the right direction of each wolf; opposite-based learning (OBL) maintains a good and diverse population; local search mechanism for fine-tuning is unlisted.	ED [43].
Opposition-Based Grey Wolf Optimizer (OGWO)	OBL is incorporated to find a better candidate solution.	Mathematical benchmark and ED [44].
Inspired Grey Wolf Optimizer (In-GWO)	Logarithmic decay characteristics of parameter 'α' are introduced and the position updating mechanism is carried out based on *pbest* and *gbest* of PSO.	Mathematical benchmark, pressure vessel design, welded beam design, spring design, and load forecasting [45]
Binary Hybrid GWO and PSO (BGWOPSO)	A binary version of hybrid GWO and PSO is utilized here.	18 standard University of California Irvine (UCI) benchmark datasets [46].
B–GWO	GWO is hybridized with β–hill climbing.	ED [47].
Orthogonal Grey Wolf Optimizer (Or-GWO)	Orthogonal Array Design (OAD) is incorporated for updating the position of leader wolves.	Mathematical benchmark and clustering datasets [48].
Accelerated Grey Wolf Optimizer (A-GWO)	An acceleration factor and uniform distribution are used to boost exploration and exploitation.	Mathematical benchmark, gear design, frequency modulated, beam design, and cost minimization of a life support system [49].
Grey Wolf Optimizer Based on Weighted Distance (GWO-WD)	The weighted distance concept is used to modify the position-updating mechanism; elimination and repositioning strategy is employed to reposition the worst search agents.	Mathematical benchmark, pressure vessel design, welded beam design, and gear design [50].

Work in [51] combines the concept of quasi-opposition-based learning with GWO for solving ED problems. However, the strategy is only used for conventional generators, and no prior testing is performed on benchmark functions. In this paper, an efficient and novel version of GWO has been proposed, namely modified quasi-opposition-based grey wolf optimization (mQOGWO), which includes (i) quasi-opposition-based learning and (ii) a sinusoidal truncated function for variable $'\alpha'$ in GWO. Quasi-opposition-based learning is applied to increase the convergence speed and the non-linear variation in $'\alpha\ '$ is adopted for a better trade-off between the exploration and exploitation of the objective function. To analyze the effectiveness of the proposed approach, it is tested on (i) 23 mathematical benchmark functions and (ii) economic dispatch (ED) problems of 15, 40, and 140 power-generating units and a microgrid problem with different energy sources.

The layout of MG consists of diesel generators, fuel cells, and wind turbine generators schematically illustrated in Figure 1.

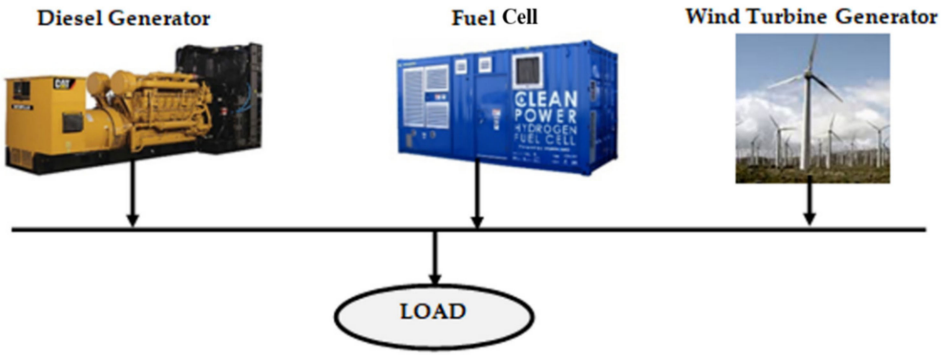

Figure 1. The layout of MG.

The remaining paper is structured as follows. Section 2 describes the formulation of the ED problem and MG. In Section 3, the working of GWO, IGWO [52], and the proposed mQOGWO is explained. The simulation results are discussed in Section 4, which includes a description of test cases and a comparative study of outcomes. Finally, the conclusions of this paper are compiled in Section 5.

2. Problem Formulation

2.1. Economic Dispatch Problem

The objective function of the ED problem for operational cost is represented as:

$$Minimise\ F_t^{Cost} = \sum_{i=1}^{N_g} f_i(P_i) \tag{1}$$

where

$$f_i(P_i) = c_i P_i^2 + b_i\ P_i + a_i;\quad i = 1, 2, 3 \ldots N_g \tag{2}$$

Considering the valve point loading (VPL) effect, the cost function can be written as:

$$f_i(P_i) = c_i P_i^2 + b_i\ P_i + a_i + \left| e_i \sin\left(f_i\left(P_i^{min} - P_i \right) \right) \right| \tag{3}$$

Here, P_i is the active power output and a_i, b_i, c_i, e_i, and f_i are cost coefficients of the i^{th} generating unit. P_i^{min} is the minimum power output of the i^{th} generating unit.

F_t^{Cost} should be minimized and subjected to the following operational constraints:

(*i*) *Power Balance*

$$\sum_{i=1}^{N_g} P_i = P_d + P_l \tag{4}$$

Using Kron's formula, P_l can be calculated as:

$$P_l = \sum_{i=1}^{N_g} \sum_{j=1}^{N_g} P_i B_{ij} P_j + \sum_{i=1}^{N_g} B_{i0}\ P_i + B_{00} \tag{5}$$

Here, P_d is the power demand, P_l is the power loss and B_{ij}, B_{i0}, and B_{00} are transmission loss coefficients.

(*ii*) *Generator Capacity Limit*

$$P_i^{min} \le P_i \le P_i^{max} \quad i \in N_g \tag{6}$$

where P_i^{min} and P_i^{max} are the minimum and maximum power output of the i^{th} generating unit.

(*iii*) *Ramp Rate Limit (RRL)*

$$P_i - P_i^o \le UR_i\ ;\ \ and \quad P_i^o - P_i \le DR_i \tag{7}$$

The inclusion of ramp rate limits modifies the generator operation constraints (6) as given below:

$$max\left(P_i^{min}, P_i^o - DR_i\right) \leq P_i \leq \min(P_i^{max}, P_i^o + UR_i) \tag{8}$$

UR_i and DR_i are the upper ramp and down ramp rates for the i^{th} generating unit; P_i^o is the active power output of the i^{th} generating unit in the previous time interval compared with the time interval of P_i.

(*iv*) *Prohibited Operating Zones (POZs)*

Every generator has some fixed restricted zones due to the limitations of machine components or an instability point of view, where operation is avoided. *POZs* make the objective function discontinuous. The feasible operating zones of the generator are represented as follows:

$$P_i = \begin{cases} P_i^{min} \leq P_i \leq \underline{P}_{i.1} \\ \overline{P}_{i,j-1} \leq P_i \leq \underline{P}_{i.j;} \quad j = 2, 3, n_i \\ \overline{P}_{i,n_i} \leq P_i \leq P_i^{max} \end{cases} \tag{9}$$

$\underline{P}_{i.j}$ and $\overline{P}_{i,j}$ are the lower and upper limits of the j^{th} prohibited zone for the i^{th} unit and n_i is the number of prohibited zones of the unit i. P_i^{min} and P_i^{max} are the maximum and minimum power outputs of the i^{th} generating unit.

2.2. The Microgrid Scheduling Problem

The microgrid problem considered for analysis combines diesel generators, fuel cells, and wind turbines as energy resources. It is tested for the optimal generation schedule with dynamic load variation over 24 h of a day.

The fuel cost of diesel generators is a convex polynomial expressed as in (10):

$$C_D(P) = \sum_{t=1}^{24} \sum_{i=1}^{\mathrm{Nd}} \left\{ c_i \times P_i^2(t) + b_i \times P_i(t) + a_i \right\} \quad \mathrm{i} = 1, 2, \ldots\ldots \mathrm{Nd} \tag{10}$$

where a_i, b_i, and c_i are the cost coefficients of the i^{th} generator producing power P_i.

The fuel cell is among the most efficient systems that utilize hydrogen energy for power generation (P_{FC}). The cost of fuel cells is dependent on the efficiency of the fuel cell (η_p) and cost coefficient (β_p), represented as [53]:

$$C_{FC}(P_{FC}) = \sum_{t=1}^{24} \left(\beta_p \sum_{p=1}^{\mathrm{Nf}} \frac{P_{FC,it}}{\eta_p} \right) \quad \mathrm{p} = 1, 2, \ldots\ldots \mathrm{Nf} \tag{11}$$

The power output for wind turbine units is dependent on wind speed, which is stochastic. In the literature, the authors of [54] show that the wind speed profile at a given location follows a Weibull distribution over time, which is given by (12).

$$f_v(v) = \left(\frac{k}{c}\right)\left(\frac{v}{c}\right)^{k-1} e^{-(vc)^k} \quad 0 < v < \infty \tag{12}$$

The output for a wind power system with a given wind velocity (P_W) is given by (13):

$$P_W = \begin{cases} 0 & \text{For} \quad 0 \leq v < v_{ci} \,\&\, v > v_{co} \\ Wrated\left(\frac{v - v_{ci}}{v_r - v_{ci}}\right) & \text{For} \quad 0 \leq v < v_{ci} \\ Wrated & \text{For} \quad v_r \leq v < v_{co} \end{cases} \tag{13}$$

where *Wrated* is the rated capacity of the wind turbine, v_{ci} is the cut-in velocity, v_{co} is the cut-out velocity, v_r is the rated velocity, and v is the wind velocity (in m/s). Cost calculation

for wind power units $(C_W(P_W))$ is given as (14), where β_W is the cost coefficient of the wind power output.

$$C_W(P_W) = \sum_{t=1}^{24} \left(\beta_W \sum_{q=1}^{\mathrm{Nw}} P_W \right) \quad \mathrm{q} = 1, 2, \ldots\ldots \mathrm{Nw} \tag{14}$$

The objective of the MG scheduling problem is to minimize the total operational cost to an optimal cost, which is expressed as [53]:

$$Min(C) = C_D(P) + C_{FC}(P_{FC}) + C_W(P_W) \tag{15}$$

3. Optimization

3.1. Grey Wolf Optimizer

GWO is a population-based optimization technique that is an SIA, with four types—alpha, beta, delta, and omega. Its analytical model imitates collective group behavior as well the leadership hierarchy of grey wolves when hunting prey. The position of the grey wolf signifies distinct position variables, and the distance between the prey and the wolf helps to obtain the fitness value of the objective function. As the simulation progresses, the wolf changes position and moves closer to the best position.

Three phases demonstrate the well-organized collective behavior of GWO: (i) entrapment of prey, (ii) hunting of prey, and (iii) attacking the prey to reach prey via the shortest route.

I. Entrapment of Prey

The initial population is generated randomly within the upper limit (*UL*) and the lower limit (*LL*).

Initially, $\mathcal{X}(t)$ denotes the current position of a wolf and its updated position to encircle the prey positioned at $\mathcal{X}_P(t)$, computed by adjusting vectors $\mathcal{A}$ and $\mathcal{C}$. The r_1 and r_2 of each $\in (0, 1)$ are the random vectors that help wolves to adjust the values of $\mathcal{A}$ and $\mathcal{C}$. The updated position $(t+1)$ and the initial phase of GWO are controlled using (16)–(19).

$$\mathcal{X}(t+1) = \mathcal{X}_P(t) - \mathcal{A} \times \mathcal{D} \tag{16}$$

where

$$\mathcal{A} = 2\alpha \mathrm{r}_1 - \alpha \tag{17}$$

$$\mathcal{D} = |\mathcal{C} \times \mathcal{X}_P(t) - \mathcal{X}(t)| \tag{18}$$

$$\mathcal{C} = 2\mathrm{r}_2 \tag{19}$$

II. Hunting of Prey

In the leadership hierarchy, the alpha wolf is supposed to be the nearest one (best solution), followed by the beta and gamma wolf. The position of the omega will vary as per the current best position. The final position is defined concerning the position of alpha, beta, and delta in the search space, and it is represented as below:

$$\mathcal{X}(t+1) = \frac{1}{3} \times (\mathcal{X}_1 + \mathcal{X}_2 + \mathcal{X}_3) \tag{20}$$

where

$$\mathcal{X}_1 = \mathcal{X}_\alpha(t) - \mathcal{A}_1 \times \mathcal{D}_\alpha, \ \ \mathcal{X}_2 = \mathcal{X}_\beta(t) - \mathcal{A}_2 \times \mathcal{D}_\beta, \ \mathcal{X}_3 = \mathcal{X}_\delta(t) - \mathcal{A}_3 \times \mathcal{D}_\delta \tag{21}$$

and

$$\mathcal{D}_\alpha = |\mathcal{C}_1.\mathcal{X}_\alpha - \mathcal{X}|, \ \mathcal{D}_\beta = \left|\mathcal{C}_2.\mathcal{X}_\beta - \mathcal{X}\right|, \ \mathcal{D}_\delta = |\mathcal{C}_3.\mathcal{X}_\delta - \mathcal{X}| \tag{22}$$

III. Attacking the Prey

This is the last phase of optimization, which takes place after the location of the prey is identified, and the wolf approaches to attack it. This approach is mathematically simulated by varying parameter 'α', using (23). 'α' is the crucial parameter in GWO that decreases from 2 to 0 linearly as iteration progresses and is mainly responsible for the exploration and exploitation of the search space.

$$\alpha = 2 - (t).\left(\frac{2}{T}\right) \tag{23}$$

The steps associated with GWO are as below:

- Search agent position vectors are initialized randomly within the lower and upper limits.
- The fitness value of each agent is evaluated based on three categories of wolves (alpha, beta, and delta) among the population. They adjust their position to catch the prey using $\mathcal{D}_\alpha$, $\mathcal{D}_\beta$ and $\mathcal{D}_\delta$, as per (22).
- Search agents update their position by (23).
- The steps of fitness calculation and update mechanism are repeated to reach the specified termination criteria.

3.2. Intelligent Grey Wolf Optimizer

Intelligent GWO (IGWO) is a variant of GWO that utilizes two mathematical frameworks: (i) an opposition-based learning (OBL) mechanism for better exploration and exploitation, and (ii) a sinusoidal truncated function for variable 'α' [52].

The OBL mechanism helps improve the convergence of a population-based algorithm [55] and utilizes the concept of opposite numbers and points. The opposite number is a mirror point of the solution in terms of extreme points. They are the lower limit (LL), the upper limit (UL), and the center of the search space, denoted as:

$$\chi^o = LL + UL - \chi \tag{24}$$

For the point P $(\chi_1, \chi_2, \ldots \chi_i \ldots \chi_d)$, its opposite point $OP\left(\chi_1^o, \chi_2^o \ldots \chi_i^0 \ldots . \chi_d^o\right)$ is expressed as [55]:

$$\chi_i^o = LL_i + UL_i - \chi_i \ \forall \tag{25}$$

where d is the dimension of search space.

In IGWO, search agent positions are initialized randomly using half of the population and the remaining using the opposite population. Here, the movement of the wolf is controlled by parameter 'α' that utilizes the truncated sinusoidal function represented as:

$$\alpha = 2 \times \left(1 - sin^2 \frac{\varnothing}{2}\right) \tag{26}$$

where

$$\varnothing = \pi \times \frac{Current\ iteration}{Max\ iteration} \tag{27}$$

3.3. Modified Quasi-Opposition-Based Grey Wolf Optimization (mQOGWO)

Two mathematical concepts, (i) quasi-opposition-based learning and (ii) a non-linear decreasing function 'a', are incorporated in basic GWO,

(*i*) *Quasi-Opposition-Based Learning*

Quasi-opposition-based learning (QOBL) is a modified version of OBL and is more effective than OBL [56,57]. The quasi-opposite number (χ^{qo}), between the center of the search space and the opposite number, is denoted as:

$$\chi^{qo} = rand\left(\frac{LL + UL}{2}, \chi^o\right) \tag{28}$$

Similarly, quasi-opposite point (χ_i^{qo}) in the d dimensional search space is denoted as:

$$\chi_i^{qo} = rand\left(\frac{LL_i + UL_i}{2}, \chi_i^o\right) \qquad for\ i = 1, 2, 3 \ldots\ldots\ldots\ldots\ldots d \tag{29}$$

(*ii*) *Non-Linear Decreasing Function 'a'*

Instead of linearly decreasing "α" as given in (23), a non-linear decreasing control strategy is used in this proposed algorithm. This newly updated function "α" is represented as (30):

$$a = 2 \cdot \left(1 - \left(\frac{Current\ iteration}{Max\ iteration}\right)^m\right)^n \tag{30}$$

For simulation purposes, m = 3.98 and n = 3.9 are considered here [58].

Figure 2 illustrates the effect of "α" on convergence using three different types of functions used for GWO, IGWO, and mQOGWO over 500 iterations.

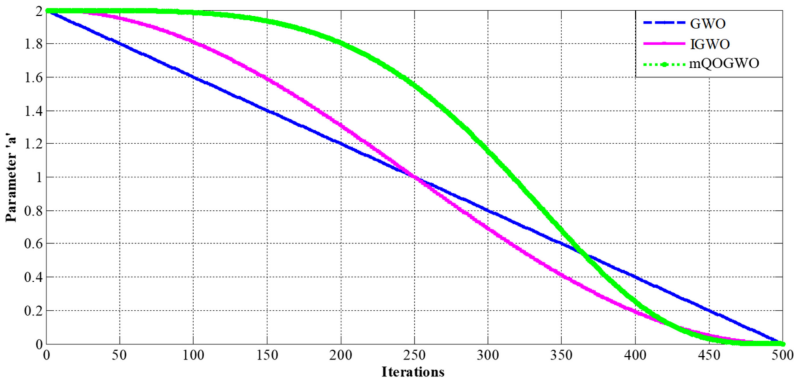

Figure 2. Variation in parameter 'α' for different algorithms.

4. Simulation Results

To analyze the feasibility, GWO, IGWO and the proposed mQOGWO are applied and tested in two sections. The first section deals with mathematical benchmarks, and the second deals with four practical cases of ED problems with different dimensions and complexity levels. The program has been written in MATLAB R2013a and executed on an Intel core i7 processor with a 3.40 GHz computer with 2 GB RAM. For the simulation analysis, the number of search agents was considered 30 for mathematical benchmarks and 100 for ED problems, respectively.

4.1. Mathematical Benchmark Functions

It contains classical mathematical benchmark functions, including unimodal, multimodal, and fixed-dimension benchmarks [59,60]. These are the minimization functions listed in Appendix A as Tables A1 and A2. *dim* represents the dimension of the problem, *range* is the upper and lower limits of the search space and f_{min} represents the optimum value of the function. For each benchmark function with a fixed dimension, proposed algorithms were run for 30 repeated trials. The statistical results in terms of the average value (Ave) and the standard deviation (SD) are tabulated in Table 2 for unimodal and Table 3 for multimodal functions. To analyze the effect of the proposed modification in the exploration and exploitation phases, all three variants, i.e., GWO, IGWO, and mQOGWO, are applied to each benchmark, and a fair comparison of the convergence curves is drawn, presented in Figures 3–5, respectively. The 3D plot gives the graphical interpretation of all the functions and the convergence curves indicate the speed and the optimum average values. Table 4 shows the $wilcoxon\ p-value$ of mQOGWO with respect to GWO and IGWO for benchmark functions, which defines the statistical uniqueness of the proposed algorithm. A significance level of 5% is selected, and a $wilcoxon\ p-value$ less than 0.05 implies the superiority of one algorithm over the other.

Table 2. Results of the unimodal and multimodal benchmark functions.

	Unimodal Benchmark											
f	mQOGWO		IGWO [52]		GWO [13]		PSO [13]		GSA [13]		DE [13]	
	Ave	SD	Ave	SD	Ave	SD	Ave	SD	Ave	SD	Ave	SD
F_1	0	0	5.55×10^{-26}	1.00×10^{-25}	6.59×10^{-28}	6.34×10^{-5}	0.000136	0.000202	5.30×10^{-17}	9.67×10^{-17}	8.20×10^{-14}	5.90×10^{-14}
F_2	1.39×10^{-200}	0	7.75×10^{-16}	7.82×10^{-16}	7.18×10^{-17}	0.029014	0.042144	0.045421	0.055655	0.194074	1.50×10^{-9}	9.90×10^{-10}
F_3	0	0	9.93×10^{-5}	0.000763	3.29×10^{-6}	79.14958	70.12562	22.11924	896.5347	318.9559	6.80×10^{-11}	7.40×10^{-11}
F_4	3.08×10^{-176}	0	1.08×10^{-6}	1.05×10^{-6}	5.61×10^{-7}	1.315088	1.086481	0.317039	7.35487	1.741452	0	0
F_5	25.7884	0.1090	27.0042	0.642515	26.81258	69.90499	96.71832	60.11559	67.54309	62.2253	0	0
F_6	0.7541	0.0818	0.6677	0.31327	0.816579	0.000126	0.000102	8.28×10^{-5}	2.50×10^{-16}	1.74×10^{-16}	0	0
F_7	7.983×10^{-5}	1.27×10^{-5}	0.00182	0.001074	0.002213	0.100286	0.122854	0.044957	0.089441	0.04339	0.00463	0.0012
	Multimodal Benchmark											
F_8	−4614.8	261.8496	−5991.23	950.3294	−6123.1	−4087.44	−4841.29	1152.814	−2821.07	493.0375	−11,080.1	574.7
F_9	0	0	1.270284	2 2.7344	0.310521	47.35612	46.70423	11.62938	25.96841	7.47006	69.2	38.8
F_{10}	2.664×10^{-15}	3.243×10^{-16}	1.64×10^{-13}	44.31×10^{-14}	1.06×10^{-13}	0.020734	0.276015	0.50901	0.062087	0.23628	9.70×10^{-8}	4.20×10^{-8}
F_{11}	0	0	0.001994	0.005099	0.004485	0.006659	0.009215	0.007724	27.70154	5.040343	0	0
F_{12}	0.0481	0.0036	0.042402	0.052673	0.053438	0.020734	0.006917	0.026301	1.799617	0.95114	7.90×10^{-15}	8.00×10^{-15}
F_{13}	0.7591	0.0618	0.551296	0.21782	0.654464	0.004474	0.006675	0.008907	8.899084	7.126241	5.10×10^{-14}	4.80×10^{-14}

Table 3. Results of fixed-dimension benchmark functions.

Fixed Dimension Benchmark												
f	mQGWO		IGWO [52]		GWO [13]		PSO [13]		GSA [13]		DE [13]	
	Ave	SD	Ave	SD	Ave	SD	Ave	SD	Ave	SD	Ave	SD
F_{14}	4.6806	0.8197	4.038	3.7415	4.0424	4.2527	3.6271	2.5608	5.8598	3.8312	0.99	3.3×10^{-16}
F_{15}	4.054×10^{-4}	1.760×10^{-5}	4.158×10^{-4}	1.813×10^{-5}	0.000337	0.000625	0.000577	0.000222	0.003673	0.001647	4.50×10^{-14}	0.00033
F_{16}	−1.0316	1.4024×10^{-5}	−1.0316	7.765×10^{-12}	−1.03163	−1.03163	−1.03163	6.25×10^{-16}	−1.03163	4.88×10^{-16}	−1.03163	3.1×10^{-13}
F_{17}	0.3982	1.7518×10^{-4}	0.3993	5.156×10^{-6}	0.397889	0.397887	0.397887	0	0.397887	0	0.397887	9.9×10^{-9}
F_{18}	3.0000	3.9096×10^{-6}	3.0000	7.693×10^{-6}	3.000028	3	3	1.33×10^{-15}	3	4.17×10^{-15}	3	2×10^{-15}
F_{19}	−3.8616	3.6947×10^{-4}	−3.8614	4.054×10^{-4}	−3.86263	−3.86278	−3.86278	2.58×10^{-15}	−3.86278	2.29×10^{-15}	N/A	N/A
F_{20}	−3.2735	0.0119	−3.2453	0.0139	−3.28654	−3.25056	−3.26634	0.060516	−3.31778	0.023081	N/A	N/A
F_{21}	−10.1532	3.6926×10^{-11}	−10.1532	2.583×10^{-8}	−10.1514	−9.14015	−6.8651	3.019644	−5.95512	3.737079	−10.1532	0
F_{22}	−10.4029	3.2452×10^{-11}	−10.4029	4.353×10^{-8}	−10.4015	−8.58441	−8.45653	3.087094	−9.68447	2.014088	−10.4029	3.9×10^{-7}
F_{23}	−10.5364	2.0493×10^{-11}	−10.3561	0.1772	−10.5343	−8.55899	−9.95291	1.782786	−10.5364	2.60×10^{-15}	−10.5364	1.9×10^{-7}

Table 4. Wilcoxon p-values comparison of mQOGWO with IGWO and GWO on benchmark functions.

Functions		F1	F2	F3	F4	F5	F6	F7		
IGWO	Unimodal	7.06×10^{-18}	5.01×10^{-11}	9.06×10^{-8}	1.12×10^{-10}	3.59×10^{-5}	3.50×10^{-9}	0.0156		
GWO		2.56×10^{-34}	3.02×10^{-11}	3.82×10^{-9}	7.44×10^{-9}	4.64×10^{-5}	1.43×10^{-8}	6.07×10^{-11}		
Functions		F8	F9	F10	F11	F12	F13			
IGWO	Multimodal	0.0079	0.011	7.93×10^{-13}	0.0214	1.29×10^{-9}	4.08×10^{-11}			
GWO		3.52×10^{-7}	1.19×10^{-12}	1.15×10^{-12}	0.0215	5.00×10^{-9}	3.16×10^{-10}			
Functions		F14	F15	F16	F17	F18	F19	F20	F21	F22
IGWO	Fixed Dimension	0.0029	0.0212	2.62×10^{-5}	0.0173	0.0292	0.03478	0.0121	0.0344	0.0044
GWO		0.0059	0.0042	5.35×10^{-6}	0.0221	0.0109	0.02789	0.0288	1.24×10^{-7}	6.47×10^{-8}

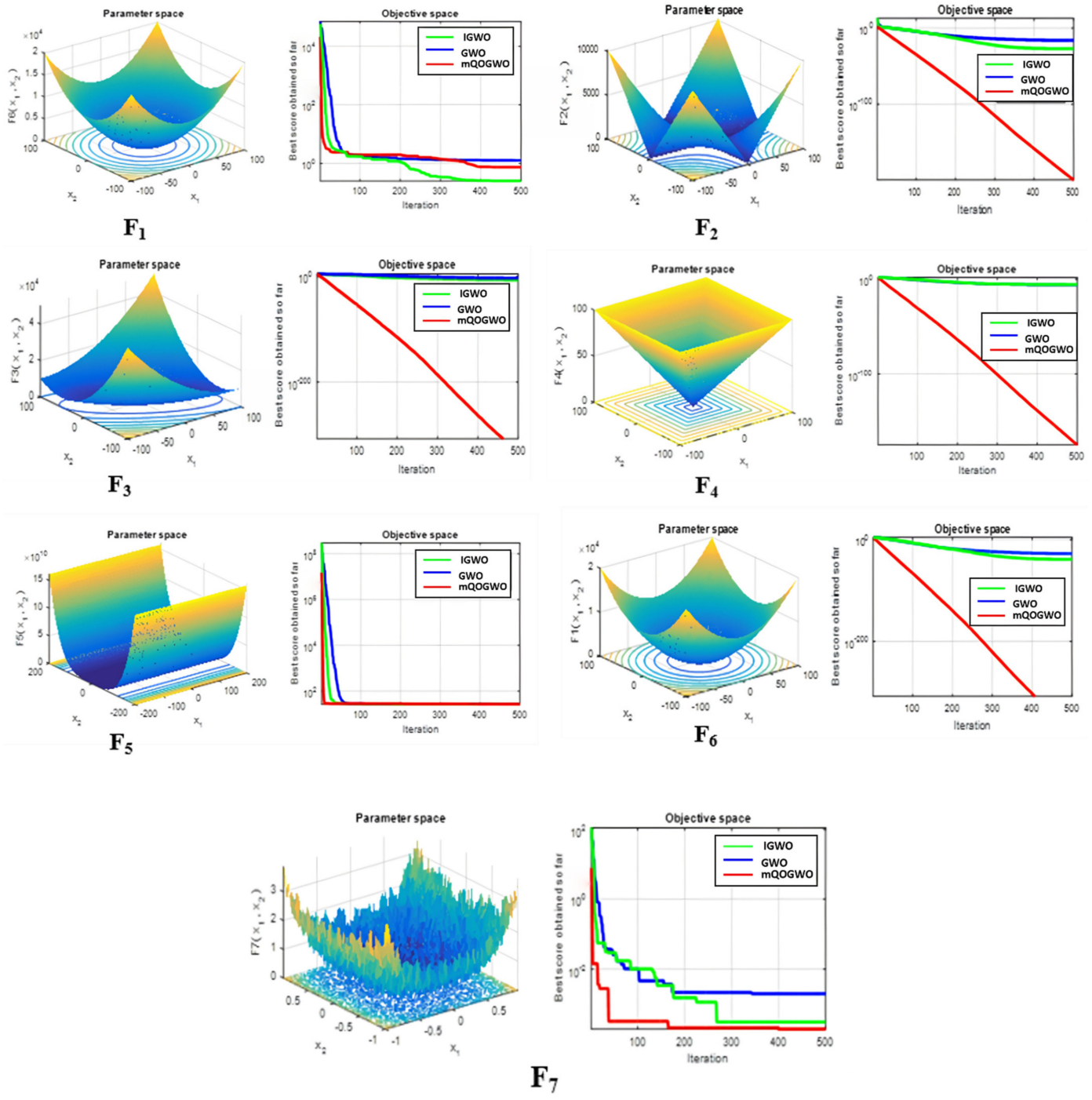

Figure 3. A 3D plot of the unimodal function and a comparison of the convergence curves.

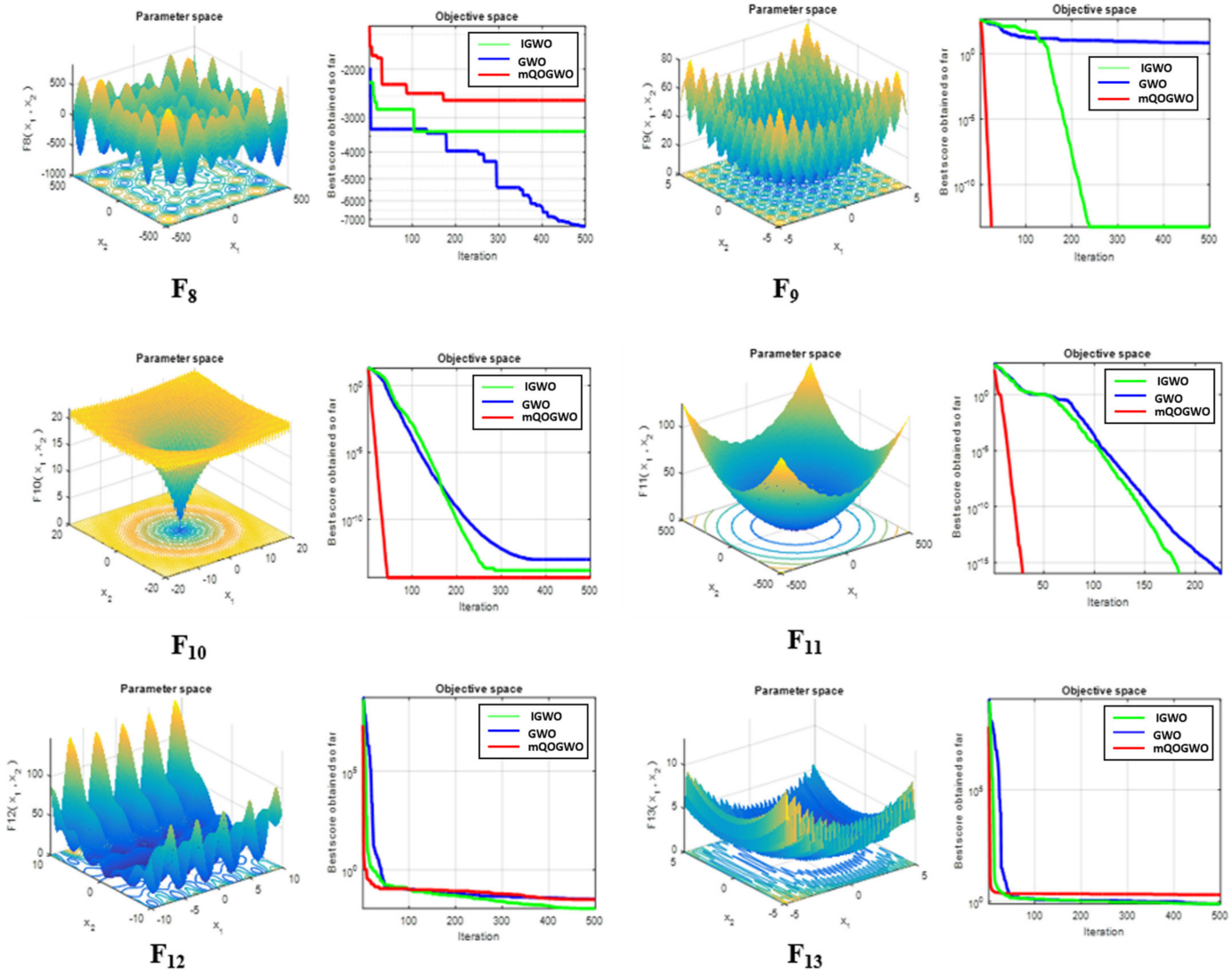

Figure 4. A 3D plot of the multimodal function and a comparison of the convergence curves.

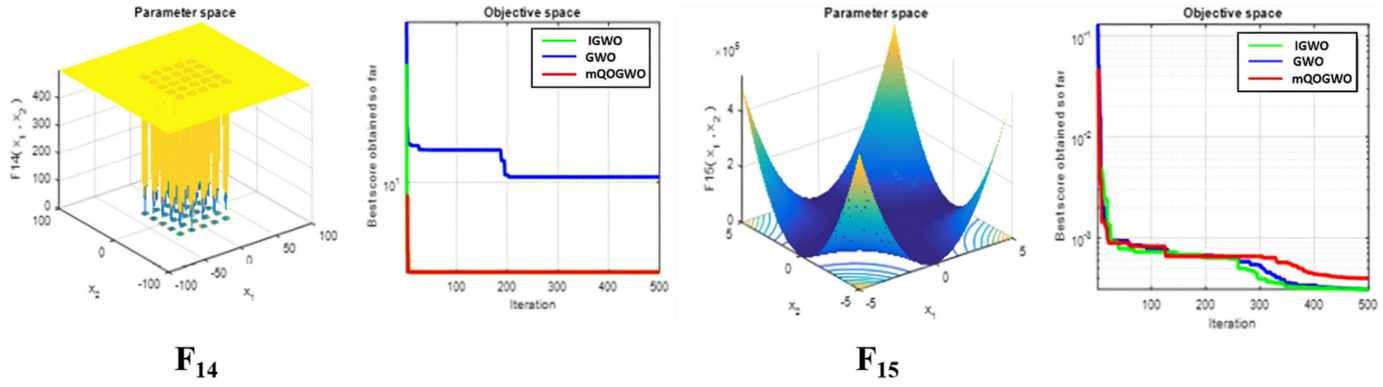

Figure 5. *Cont.*

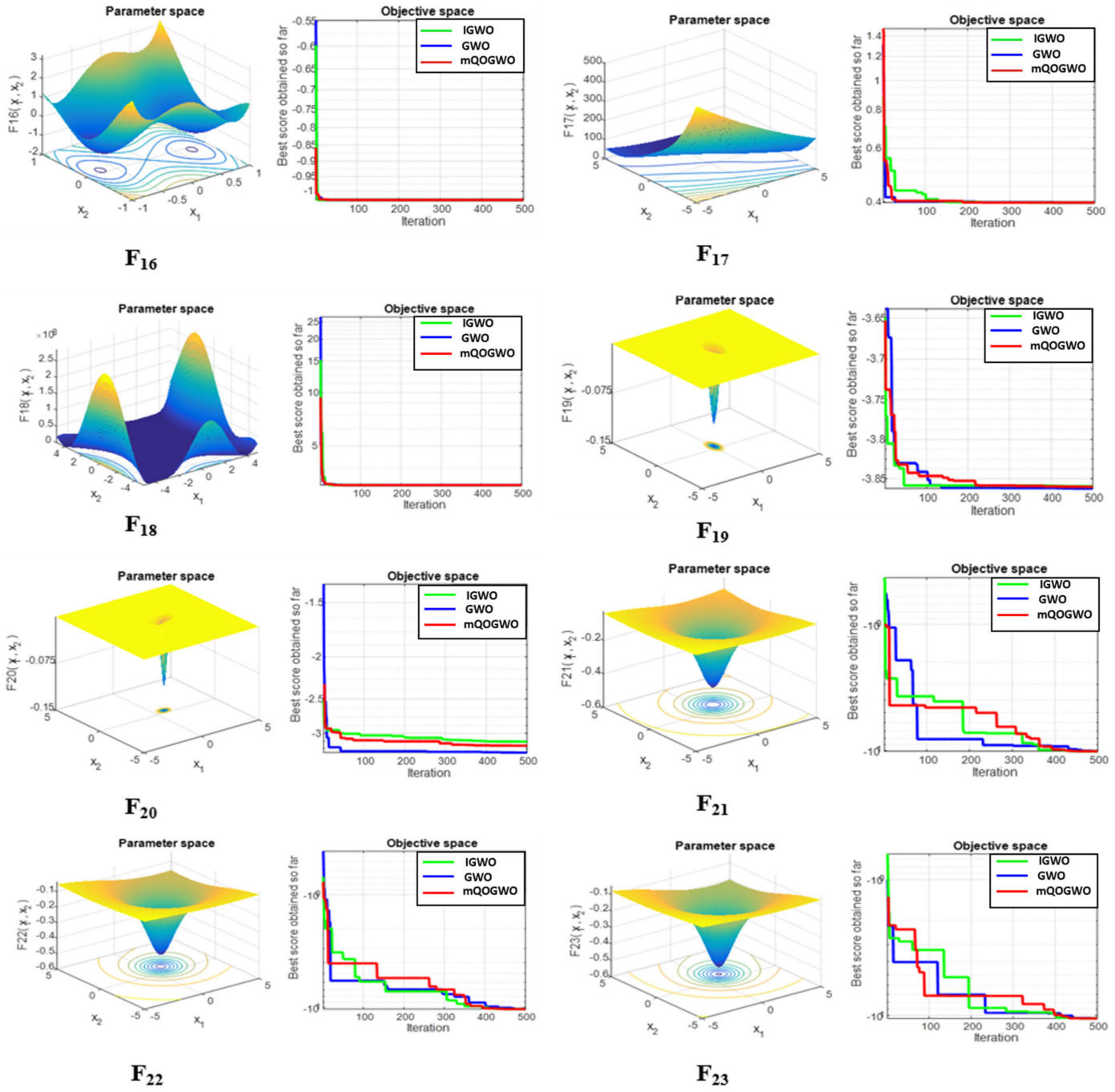

Figure 5. A 3D plot of the fixed-dimension function and a comparison of the convergence curves.

4.2. Economic Dispatch Problems

The proposed mQOGWO, IGWO, and GWO algorithms have been applied to solve ED problems. Four test systems are considered here for analysis with different dimensions and complexity. Test system I, II, and III are analyzed with a fixed load demand, whereas test system IV is a microgrid analyzed with dynamic variation in load demand over 24 h of a day.

Test System I: A 15 Unit System

This problem has fifteen thermal generating units with convex fuel cost characteristics. The total load demand of the system is considered as 2630 MW. The generator data and B-loss coefficient matrix are taken similarly to [40]. The complexity such as ramp rate

limits (RRLs) and prohibited operating zones, which makes the system discontinuous, are also considered here. The comparison of the cost convergence curves obtained using the above three algorithms is illustrated in Figure 6. After the 30 repeated trials, the statistical comparison of operational costs is presented in Table 5. The optimal generation schedule corresponding to the best cost is listed in Appendix A Table A3. Table A3 shows that all three variants efficiently manage the specified operational constraints.

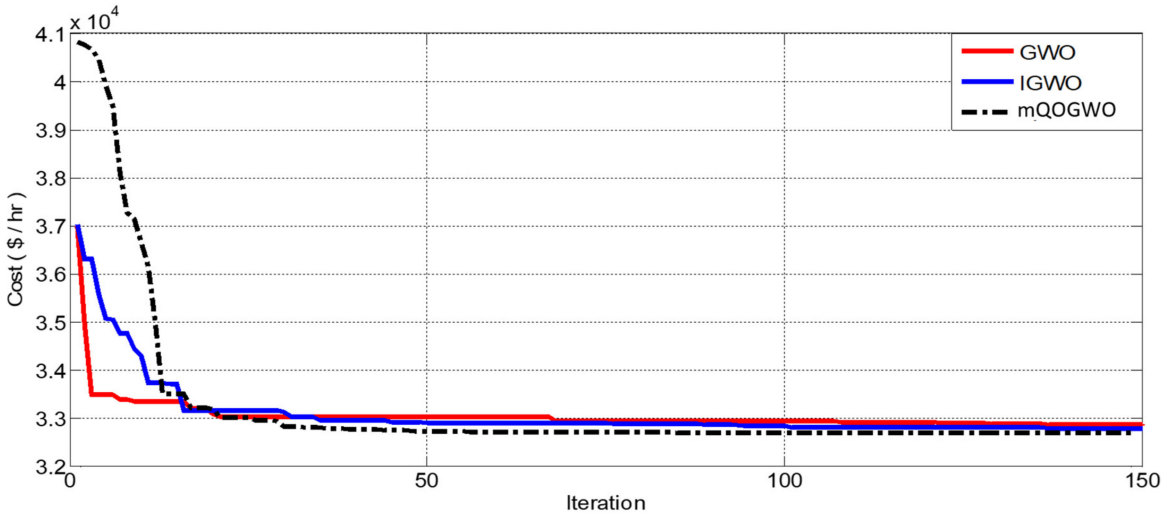

Figure 6. Convergence curves for QOGWO, IGWO, and GWO for test system I.

Test System II: A 40 Unit System

The system contains forty thermal generating units with valve point loading (VPL) effects. VPL makes the function multimodal and non-convex in nature. The fuel cost coefficient data of generating units is adopted from [39]. The total load demand on the system is 10,500 MW. The transmission loss is also considered here [61]. The optimal generation schedule, including loss, is presented in Appendix A Table A4. Here, the operational constraints associated with it are fully satisfied. The statistical comparison of costs is presented in Table 6. The comparison of cost convergence curves obtained by GWO, IGWO, and mQOGWO is represented in Figure 7.

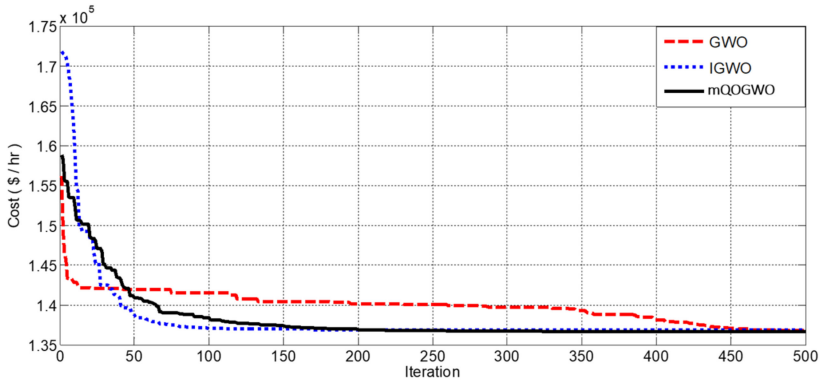

Figure 7. Convergence curves for QOGWO, IGWO, and GWO for test system II.

Test System III: A 140 Unit System (Korean Power System)

Experiments are conducted on the Korean power system to investigate the feasibility of the proposed algorithm for large-scale power systems [62]. This system is analyzed under two operating conditions. Test system III-A contains one hundred and forty thermal generating units with convex characteristics as given in (2) with RRLs. The total power demand is set to 49,342 MW. Test system III-B has one hundred and forty thermal generating

units with non-convex characteristics as given in (3) with RRLs and POZ constraints. As it is the largest standard test system, the three abovementioned algorithms are applied and tested over thirty repeated trials, and the statistical results are tabulated, presented in Table 6. The optimal generation schedule corresponding to the best cost solution for test systems III-A and III-B are shown in Appendix A as Tables A5 and A6, respectively.

Table 5. Comparison of the results for test system I (a *15 unit system*).

Methods	Min Cost (USD/h)	Ave Cost (USD/h)	Max Cost (USD/h)	SD	Ave CPU Time (s)
AIS [63]	32,854.00	32,873.25	32,892.00	10.81	NA
SA [64]	32,786.40	32,869.51	33,038.95	112.32	71.25
GA [64]	32,779.81	32,841.21	33,041.64	81.22	48.17
TSA [64]	32,762.12	32,822.84	33,041.64	60.59	26.41
PSO [64]	32,724.17	32,807.45	32,841.38	21.24	13.25
MTS [64]	32,716.87	32,767.21	32,796.15	17.51	3.65
DSPSO-TSA [65]	32,715.06	32,724.63	32,730.39	8.40	2.30
Jaya [66]	32,712.65	32,743.46	32,822.99	47.03	3.80
Jaya-SML [66]	32,706.36	32,706.68	32,707.29	2.32	5.14
CJaYa [67]	32,710.08	32,740.07	32,828.66	NA	NA
MP-Cjaya [67]	32,706.52	32,706.72	32,708.87	NA	NA
GWO	32,702.12	32,703.31	32,704.58	1.48	8.23
IGWO	32,693.19	32,694.74	32,695.61	1.38	7.16
mQOGWO	**32,692.23**	**32,692.40**	**32,692.60**	**1.09**	**3.28**

Table 6. Comparison of the results for test system II (a *40 unit system*).

Methods	Min Cost (USD/h)	Ave Cost (USD/h)	Max Cost (USD/h)	SD	Ave CPU Time (s)
HGWO [39]	136,681.00	136,684	NA	NA	NA
OGWO [44]	136,440.62	136,442.26	136,445.98	0.1003	NA
BBO [68]	137,026.82	137,116.58	137,587.82	NA	40.00
DE/BBO [68]	136,950.77	136,966.77	137,150.77	NA	32.00
ORCCRO [69]	136,855.19	136,855.19	136,855.19	NA	14.00
SCA [69]	136,653.02	136,653.02	136,653.10	NA	28.00
OIWO [70]	136,452.68	136,452.68	136,452.68	NA	10.70
GWO	136,447.39	136,541.34	136,588.22	25.48	11.34
IGWO	136,444.30	136,462.93	136,510.15	17.12	10.78
QOGWO	**136,437.81**	**136,440.70**	**13,663.40**	**5.46**	**9.86**

Test System IV: Simulation Results of the Dynamic ED Problem of a Microgrid

Uncertain wind velocity and dynamic variation in load demand over 24 h of a day makes the makes the objective function of microgrid system probabilistic and much more complex to solve. This microgrid test system combines two diesel generators, three fuel cells, and two wind turbines as energy resources [53]. mQOGWO, IGWO, and GWO are implemented and analyzed with the number of search agents and a maximum iteration of 100. The comparison of the cost convergence of the above three algorithms is illustrated in Figure 8. For validation purposes, a comparison of the results in terms of the best cost

solution is made with the reported results using the cuckoo search algorithm (CSA) [53], differential evolution (DE) [53], and particle swarm optimization (PSO) [53] and presented in Figure 9. Here, the best operational cost of USD 30,690.42 is obtained by mQOGWO followed by USD 31,912.49 by IGWO and USD 32902.49 by GWO.

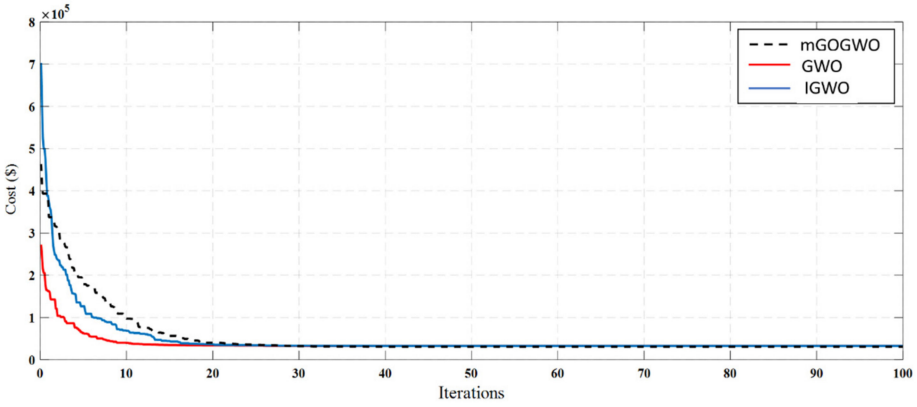

Figure 8. Convergence curves for mQOGWO, IGWO, and GWO for test system IV.

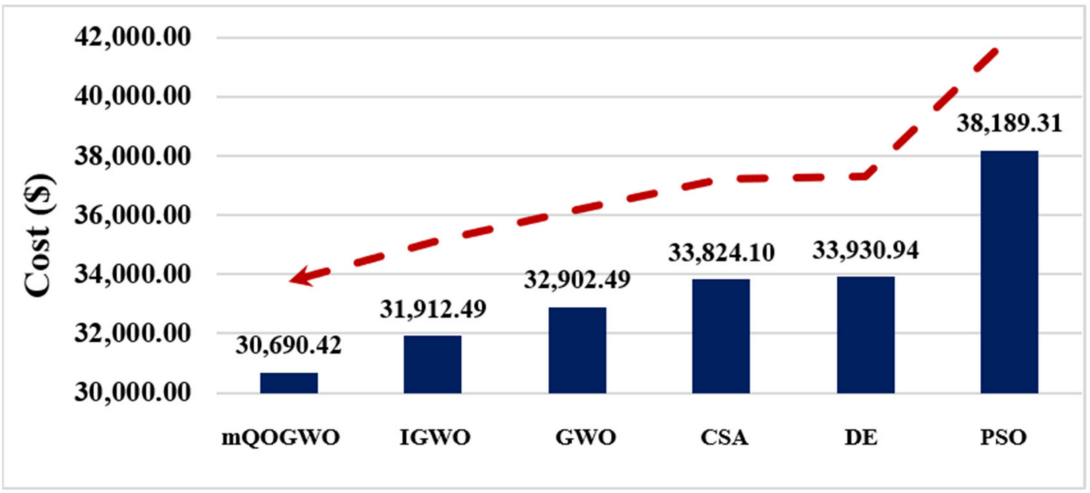

Figure 9. Comparison of the optimal cost of test system IV (DED problem of a *microgrid*) [53].

4.3. A Comparative Study

Best solutions: A comparison of the statistical results is also made in two sections. The first section deals with comparison results for benchmark functions with unimodal, multimodal, and fixed dimensions, listed in Tables 1 and 2, respectively. As GWO was initially proposed by Mirjalili [13] and IGWO by Saxena et al. [52], they have provided the statistical results for the above benchmarks and validated them with well-established methods such as DE [13] and PSO [13]. Therefore, their results are considered here for a fair comparison. After analyzing the results of the above table, it is clearly observed that mQOGWO provides the minimum average values in most of the unimodal functions (except F6). It also provides the lowest average value of benchmark functions for a few multimodal (F9 to F11) and for a few fixed-dimension functions (F21 to F23). From Figures 4 and 5, it can be seen that, in most cases, QOGWO converges faster. This shows the efficacy of QOGWO for solving single objective problems.

For the practical test system I, a comparison of the results in terms of cost and computational time is made with AIS [61], DSPSO-TSA [63], Jaya-SML [64], and MP-Cjaya [65] in Table 5. Here, the minimum cost obtained by QOGWO as 32,692.23 USD/h with a standard deviation (SD) of 1.09 USD/h is the best among all reported methods considered for comparison.

Similarly, for the 40 unit non-convex ED problem (test system II), a comparison of the results is made in Table 6 with the reported results by HGWO [39], OGWO [44], DE/BBO [67], OIWO [69] and the obtained results by GWO, IGWO, and mQOGWO. Here, even the average cost of 136,440.70 USD/h attained by mQOGWO is better than the minimum cost obtained by others.

For the large-dimension ED problem with 140 power-generating units, analysis was carried out using GWO, IGWO and mQOGWO considering convex (test system III-A) and non-convex (test system III-B) fuel cost characteristics. Table 7 shows the statistical comparison of the results with the reported results using other methods. Here, the obtained best result using mQOGWO, 1,655,679.43 USD/h, is almost comparable to that obtained with HHE [71] and CQGSO [72] but slightly inferior to the reported result by MFPA [70], 1,655,679.39 USD/h, for the convex system.

Table 7. Comparison of the results for test system III (a *140 unit system*).

Methods	Min Cost (USD/h)	Ave Cost (USD/h)	Max Cost (USD/h)	SD	Ave CPU Time (s)
Test System III-A (Convex Characteristics)					
FPA [73]	1,655,685.80	1,655,709.06	1,655,732.32	24.86	10.24
MFPA [73]	1,655,679.39	1,655,679.42	1,655,679.43	0.02	5.57
CCPSO [62]	1,655,685.00	1,655,685.00	1,655,685.00	NA	42.90
CQGSO [72]	1,655,679.43	1,655,679.43	1,655,679.43	NA	18.61
HHE [71]	1,655,679.41	NA	NA	NA	8.23
GWO	1,655,685.80	1,656,187.78	1,656,575.94	20.02	5.45
IGWO	1,655,679.57	1,655,965.60	1,656,498.17	24.9	5.54
QOGWO	**1,655,679.43**	**1,655,869.64**	**1,656,018.68**	**2.96**	**6.76**
Test System III-B (Non-Convex Characteristics)					
GSO [72]	1,728,151.17	1,745,515.00	1,753,229.56	NA	NA
BBO [68]	1,665,478.25	1,667,548.32	1,669,536.35	NA	NA
DE/BBO [68]	1,660,215.65	1,661,257.35	1,662,349.58	NA	NA
ORCCRO [68]	1,659,654.83	1,659,725.96	1,659,823.97	0.16	NA
SCA [69]	1,658,384.88	1,658,384.25	1,658,386.57	0.1	NA
CQGSO [72]	1,657,962.73	1,657,962.74	1,657,776.00	NA	31.67
CCPSO [64]	1,657,962.73	1,657,962.73	1,657,962.73	0.00	150.00
HHE [71]	1,657,962.71	NA	NA	NA	8.80
FPA [73]	1,657,962.77	1,658,051.90	1,658,570.77	228.84	12.67
MFPA [73]	1,657,962.69	1,657,962.75	1,657,962.82	0.06	5.71
GWO	1,657,962.89	1,658,612.89	1,659,262.89	40.11	5.70
IGWO	1,657,962.76	1,658,027.76	1,658,092.76	25.31	5.75
QOGWO	**1,657,962.73**	**1,657,969.23**	**1,657,975.73**	**4.03**	**6.89**

For the non-convex objective function, with RRLs and POZ, test system III-B, the best cost solution of QOGWO is 1,657,962.73 USD/h, which is similar to the reported result by CCPSO [73] and CQGSO [72]; and very close to 1657962.69 USD/h obtained by MFPA [70].

In test system IV, analysis for optimum generation scheduling of a microgrid comprised of three power-generating units is carried out with dynamic load variation over 24 h by GWO, IGWO and mQOGWO. Obtained simulation results are compared with the reported results by the CSA [53], PSO [53] and DE [53] in Figure 9. Here, a decreasing trend is clearly observed in the range of 20%–3% for PSO to IGWO while comparing the minimum cost obtained by mQOGWO as USD 30,690.42. The optimal generation schedules

obtained by GWO, IGWO are plotted in Figure A1, and that by mQOGWO is presented in Table A7.

Computational efficiency: Tables 5–7 show the average CPU time (s) of various methods for test systems I, II, and III, respectively. For the 15-unit ED problem (Test systems I), QOGWO takes 3.28 s, which is comparable to 3.65 s by MTS [62] and 3.80 s by Jaya [64] but inferior to 2.80 s by DSPSO-TSA [63].

The average CPU time obtained by mQOGWO is 9.86 s for the forty-unit non-convex system with transmission loss. Considering the dimension and complexity of test system II, this computational time is quite obvious.

For test system III, with 140 power-generating units, a minimum computational time of 8.24 s by mQOGWO is superior then that of 31.67 s by CQGSO [72] and 12.67 s by FPA [70] but inferior to 5.71 s by MFPA [70].

From Figure 6, it is seen that QOGWO reaches the final value faster. It takes a smaller number of iterations to explore and start the exploitation phase earlier than GWO and IGWO. For the large-dimension non-convex test system, cost convergence was compared in Figure 7. Here, GWO and IGWO reach the exploitation phase faster than mQOGWO but have a small error in the region of the global optimal value. Comparing the computational time and the rate of convergence of QWO, IGWO, and mQOGWO for all test systems, it is evident that mQOGWO attained better results in all cases. However, the convergence rate seems to depend on system size and complexity.

Solution quality: The solution quality in this paper is compared based on (i) standard deviation, (ii) Wilcoxon's *p*-value and (iii) degree of dispersion and skewness in the box plot as below.

(*i*) *Standard deviation*

While solving classical benchmark functions, mQOGWO has shown appreciable results in terms of minimum SD. mQOGWO has an almost negligible SD for all unimodal functions. However, the results are comparable with other methods for multimodal and fixed-dimension benchmark functions.

In test system I, mQOGWO has a minimum standard deviation, which suggests the solutions obtained are more closely packed near the mean and have more precise results than others. The SD of mQOGWO for test systems II and III is not the lowest of all algorithms but it is still lower than that of GWO and IGWO when compared separately.

(*ii*) *Wilcoxon's p-value*

The statistical significance of the algorithms was calculated using the obtained results from the algorithms [74]. In this paper, the results are obtained by GWO, IGWO, and mQOGWO on 23 mathematical benchmark functions. Wilcoxon's *p*-value (probability value) is calculated after taking the results of GWO and IGWO pairwise with the mQOGWO results, tabulated in Table 4. A 5% significance level, a *p*-value of less than 0.05, implies the superiority of mQOGWO over the other two. This characteristic shows that, statistically, mQOGWO gives unique and better-quality solutions compared to GWO and IGWO.

(*iii*) *Data dispersion and skewness in the box plot*

For a more comprehensive analysis, the data dispersion and skewness of the obtained results for GWO, IGWO, and mQOGWO are compared through a box plot as illustrated in Figure 10. The box plots graphs show that the median of mQOGWO is the lowest in all four cases. The interquartile range for mQOGWO is less as compared to GWO and IGWO, which depicts less data dispersion and a more precise window for expected solutions. The median for mQOGWO is equally spaced from the first and third quartile, implying normal distribution of solution results. Additionally, the length of whiskers in Figure 10a,b,d,e for mQOGWO is equal, which implies that solution distribution is not skewed.

Comparing the solution sets for GWO, IGWO, and mQGWO on factors such as standard deviation and box plots, it is clear that solutions obtained by mQOGWO are statistically more appealing, with the least data dispersion and minimum skewness.

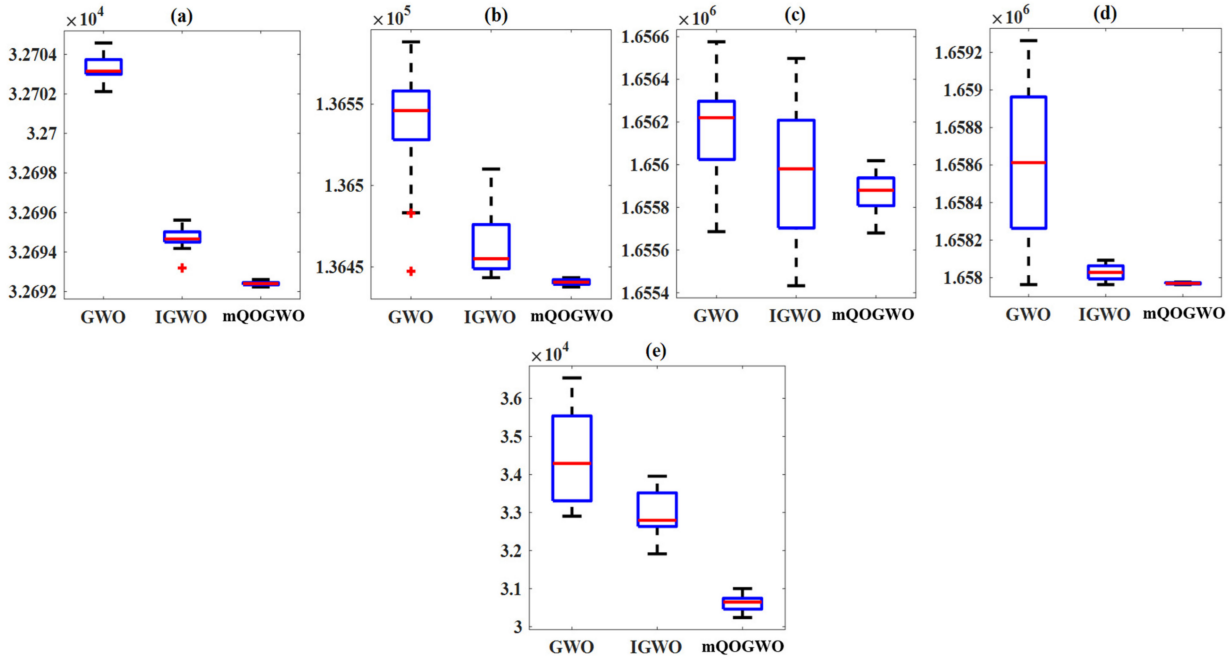

Figure 10. Box plots for (**a**) test system I, (**b**) test system II, (**c**) test system III-A, (**d**) test system III-B, and (**e**) test system IV.

5. Conclusions

In this paper, a modified quasi-opposition-based grey wolf optimization method is proposed and successfully implemented to solve mathematical benchmark, convex and non-convex ED problems, including the microgrid scheduling problem with complex operational constraints. Considering the simulation results of the proposed method for all test cases, it is evident that mQOGWO has the ability to converge to a better-quality solution. The average computation time and the statistical results are also analyzed considering the dimension and complexity of the problem, which supports its efficacy while dealing with a complex optimization problem. Application and analysis of mQOGWO on multiobjective problems can be the scope of a future study.

Author Contributions: Conceptualization, S.M.D. and H.M.D.; methodology, S.R.S.; software, S.R.S.; validation, S.M.D., H.M.D. and S.R.S.; formal analysis, S.R.S.; investigation, S.M.D.; resources, H.M.D.; data curation, S.M.D.; writing—original draft preparation, S.M.D. and H.M.D.; writing—review and editing, H.M.D. and S.R.S.; visualization, S.M.D.; supervision, H.M.D. and S.R.S.; project administration, S.M.D. and H.M.D.; funding acquisition, S.R.S. All authors have read and agreed to the published version of the manuscript.

Funding: This research was funded by "Woosong University's Academic Research Funding—2022".

Institutional Review Board Statement: Not applicable.

Informed Consent Statement: Not applicable.

Data Availability Statement: Not applicable.

Conflicts of Interest: The authors declare no conflict of interest.

Appendix A

Table A1. Unimodal and multimodal benchmark functions.

F_i	Name	Function	dim	Range	f_{min}
		Unimodal Benchmark			
F_1	*Sphere*	$f(x) = \sum_{i=1}^{n} x_i^2$	30	[−100,100]	0
F_2	*Schwefel's Problem* 2.22	$\sum_{i=1}^{n} \lvert x_i \rvert + \prod_{i=1}^{n} \lvert x_i \rvert$	30	[−10,10]	0
F_3	*Schwefel's Problem* 1.20	$\sum_{i=1}^{n} \left(\sum_{j=1}^{i} x_j \right)$	30	[−100,100]	0
F_4	*Schwefel's Problem* 2.21	$max\{\lvert x_i \rvert, 1 \le i \le n\}$	30	[−100,100]	0
F_5	*Generalized Rosenbrock*	$\sum_{i=1}^{n-1} \left[100 \left(x_{i+1} - x_i^2 \right)^2 + (x_i - 1)^2 \right]$	30	[−30,30]	0
F_6	*Step*	$\sum_{i=1}^{n} \lvert x_i + 0.5 \rvert^2$	30	[−100,100]	0
F_7	*Noise*	$\sum_{i=1}^{n} i x_i^4 + random[0,1)$	30	[−1.28,1.28]	0
		Multimodal Benchmark			
F_8	*Schwefel's* 2.26	$\sum_{i=1}^{n} -x_i \sin\left(\sqrt{\lvert x_i \rvert} \right)$	30	[−500,500]	−12,569.5
F_9	*Rastrigin*	$\sum_{i=1}^{n} \left[x_i^2 - 10\cos(2\Pi x_i) + 10 \right]$	30	[−5.12,5.12]	0
F_{10}	*Aukley*	$-20e^{\left(-0.2\sqrt{\frac{1}{n}\sum_{i=1}^{n} x_i^2}\right)} - e^{\left(\frac{1}{n}\sum_{i=1}^{n} cos2\Pi x_i\right)} + 20 + e$	30	[−32,32]	0
F_{11}	*Griewank*	$\frac{1}{4000}\sum_{i=1}^{n} x_i^2 - \prod_{i=1}^{n} cos\left(\frac{x_i}{\sqrt{i}}\right) + 1$	30	[−600,600]	0
F_{12}	*Generalized Penalized* 1	$\frac{\Pi}{n}\left\{ 10sin^2(\Pi y_i) + \sum_{i=1}^{n-1}(y_i-1)^2\left[1+10sin^2(\Pi y_{i+1})\right] + (y_n-1)^2 \right\} + \sum_{i=1}^{n} u(x_i,10,100,4)$ Where $y_i = 1 + \frac{1}{4}(x_i+1)$ and, $u(x_i,a,k,m) = \begin{cases} k(x_i-a)^m & x_i > a \\ 0 & -a < x_i < a \\ k(-x_i-a)^m & x_i < -a \end{cases}$	30	[−50,50]	0
F_{13}	*Generalized Penalized* 2	$0.1\left\{ sin^2(3\Pi x_i) + \sum_{i=1}^{n-1}(x_i-1)^2\left[1+sin^2(3\Pi x_{i+1})\right] + (x_n-1)sin^2(2\Pi x_n) \right\} + \sum_{i=1}^{n} u(x_i,5,100,4)$ were $u(x_i,a,k,m) = \begin{cases} k(x_i-a)^m & x_i > a \\ 0 & -a < x_i < a \\ k(-x_i-a)^m & x_i < -a \end{cases}$	30	[−50,50]	0

Table A2. Fixed-dimension benchmark functions.

F_i	*Name*	*Function*	*dim*	*Range*	f_{min}
		Fixed Dimension Benchmark			
F_{14}	*Shekel's Foxholes*	$f(x) = \left[\frac{1}{500} + \sum_{j=1}^{25} \frac{1}{\sum_{i=1}^{2}\left(x_i - a_{ij}\right)^6}\right]^{-1}$ where $a_{ij} = \begin{bmatrix} -32 & -16 & 0 & 16 & 32 & \cdots & \cdots & 32 & 16 & 0 & 16 & 32 \\ -32 & -32 & -32 & -32 & -32 & \cdots & \cdots & 32 & 32 & 32 & 32 & 32 \end{bmatrix}$	2	$[-65.536, 65,536]$	1
F_{15}	*Kowalik*	$f(x) = \sum_{i=1}^{11}\left[a_i + \frac{x1\left(b_i{}^2 + b_i x2\right)}{b_i^2 + b_i x3 + x4}\right]^2$ where $a_j = [\,0.1957 \quad 0.1947 \quad 0.1735 \quad 0.16 \quad 0.084 \quad 0.0627$ $0.0456 \quad 0.0342 \quad 0.0323 \quad 0.0235 \quad 0.0246]$ $b_i = [0.25 \quad 0.5 \quad 1 \quad 2 \quad 4 \quad 6 \quad 8 \quad 10 \quad 12 \quad 15 \quad 16 \quad]$	4	$[-5,5]$	0.003075
F_{16}	*Six Hump Camel Back*	$f(x) = 4x_1^2 + 2.1x_1^4 + \frac{1}{3}x_1^3 + x_1x_2 - 4x_2^2 + 4x_2^4$	2	$[-5,5]$	-1.0316285
F_{17}	*Bramin*	$f(x) = \left(x_2 - \frac{5.1}{4\Pi^2}x_1^2 + \frac{5}{\Pi}x_1\right)^2 + 10\left(1 - \frac{1}{8}\right)\cos(x_1) + 10$	2	$[-5,10]\times$ $[0,10]$	0.398
F_{18}	*Goldstein* $-$ *Price*	$f(x) = \left[1 + (x_1 + x_2 + 1)^2\left(19 - 14x_1 + 3x_1^2 - 14x_2 + 6x_1x_2 + 3x_2^2\right)\right] \times \left[30 + (2x_1 - 3x_2)^2\left(18 - 32x_1 + 12x_1^2 + 48x_2 - 36x_1x_2 + 27x_2^2\right)\right]$	2	$[-2,2]$	3
F_{19}	*Hartman's Family*	$f(x) = -\sum_{i=1}^{4} c_i exp\left[-\sum_{j=1}^{3} a_{ij}\left(x_j - p_{ij}\right)^2\right]$	4	[0,1]	-3.86
F_{20}		$f(x) = -\sum_{i=1}^{4} c_i exp\left[-\sum_{j=1}^{6} a_{ij}\left(x_j - p_{ij}\right)^2\right]$ where $a_{ij} = \begin{bmatrix} 10 & 3 & 17 & 3.5 & 1.7 & 8 \\ 0.05 & 10 & 17 & 0.1 & 8 & 14 \\ 3 & 3.5 & 1.7 & 10 & 17 & 8 \\ 17 & 8 & 0.05 & 10 & 0.1 & 14 \end{bmatrix}$, $c_i = \begin{bmatrix} 1 \\ 1.2 \\ 3 \\ 3.2 \end{bmatrix}$ $p_{ij} = \begin{bmatrix} 0.1312 & 0.1696 & 0.5569 & 0.0124 & 0.8283 & 0.5886 \\ 0.2329 & 0.4135 & 0.8307 & 0.3736 & 0.1004 & 0.9991 \\ 0.2348 & 0.1415 & 0.3522 & 0.2883 & 0.3047 & 0.6650 \\ 0.4047 & 0.8828 & 0.8732 & 0.5743 & 0.1091 & 0.0381 \end{bmatrix}$	6	[0,1]	-3.32
F_{21}	*Shekel's Family*	$f(x) = -\sum_{i=1}^{5}\left[(x - a_i)(x - a_i)^T + c_i\right]^{-1}$	4	[0,10]	-10
F_{22}		$f(x) = -\sum_{i=1}^{7}\left[(x - a_i)(x - a_i)^T + c_i\right]^{-1}$	4	[0,10]	-10
F_{23}		$f(x) = -\sum_{i=1}^{10}\left[(x - a_i)(x - a_i)^T + c_i\right]^{-1}$ $a_i = \begin{bmatrix} 4 & 1 & 8 & 6 & 3 & 2 & 5 & 8 & 6 & 7 \\ 4 & 1 & 8 & 6 & 7 & 9 & 5 & 1 & 2 & 3.6 \\ 4 & 1 & 8 & 6 & 3 & 2 & 3 & 8 & 6 & 7 \\ 4 & 1 & 8 & 6 & 7 & 9 & 3 & 1 & 2 & 3.6 \end{bmatrix}$ $c_i = [0.1 \quad 0.2 \quad 0.2 \quad 0.4 \quad 0.4 \quad 0.6 \quad 0.3 \quad 0.7 \quad 0.5 \quad 0.5\,]$	4	[0,10]	-10

Table A3. Optimal generation schedule for test system I (a *15 unit system*).

Units(MW)	mQOGWO	IGWO	GWO
P1	455.000	454.994	455.000
P2	380.000	380.003	380.000
P3	130.000	130.000	130.000
P4	130.000	130.000	130.000
P5	170.000	169.942	170.000
P6	460.000	459.999	460.000
P7	430.000	429.978	430.000
P8	69.476	87.951	116.554
P9	60.108	41.841	45.883
P10	160.000	160.000	127.412
P11	80.000	80.000	80.000
P12	80.000	80.000	80.000
P13	25.000	25.000	25.000
P14	15.000	15.001	15.000
P15	15.000	15.004	15.000
P_{loss} (MW)	29.585	29.717	29.849
F_{cost} (USD/h)	32,692.230	32,693.190	32,702.120

Table A4. Optimal generation schedule for test system II (a *40 unit system*).

Units(MW)	QOGWO	IGWO	GWO	Units	QOGWO	IGWO	GWO
P1–P3	114.00	114.00	114.00	**P21**	523.28	523.32	523.63
P4	179.73	181.37	180.12	**P22**	523.30	550.00	550.00
P5	87.80	88.18	88.81	**P23–P24**	523.28	523.28	523.28
P6	140.00	140.00	140.00	**P25**	523.28	523.30	524.44
P7–P8	300.00	300.00	300.00	**P26**	523.28	523.30	523.37
P9	289.89	300.00	300.00	**P27–P29**	10.00	10.00	10.00
P10	279.60	279.60	279.60	**P30**	87.80	87.80	87.80
P11	243.60	243.60	243.42	**P31**	190.00	190.00	190.00
P12	94.00	94.00	94.00	**P34–P35**	200.00	200.00	200.00
P13–P16	484.04	484.04	484.04	**P36**	164.80	164.80	164.80
P17–P18	489.28	489.28	489.28	**P37–P39**	110.00	110.00	110.00
P19–P20	511.28	511.28	511.30	**P40**	550.00	511.90	511.34
		Ploss (MW)			972.20	973.00	973.22
		Fcost (USD/h)			136,437.81	136,444.30	136,447.39

Table A5. Optimal generation schedule for test system III-A.

Units	QOGWO	IGWO	GWO	Units	QOGWO	IGWO	GWO
P1	119.00	119.00	119.00	**P82**	56.00	56.00	56.00
P2	164.00	164.00	164.00	**P83–P85**	115.00	115.00	115.00
P3–P6	190.00	190.00	190.00	**P86–P87**	207.00	207.00	207.00

Table A5. *Cont.*

Units	QOGWO	IGWO	GWO	Units	QOGWO	IGWO	GWO
P7–P8	490.00	490.00	490.00	**P88–P89**	175.00	175.00	175.00
P9–P12	496.00	496.00	496.00	**P90**	180.43	180.49	180.49
P13	506.00	506.00	506.00	**P91**	175.00	175.00	175.00
P14	509.00	509.00	509.00	**P92**	575.40	575.40	575.40
P15	506.00	506.00	506.00	**P93**	547.50	547.50	547.50
P16	505.00	505.00	505.00	**P94**	836.80	836.80	836.80
P17–P18	506.00	506.00	506.00	**P95**	837.50	837.50	837.50
P19–P24	505.00	505.00	505.00	**P96**	682.00	682.00	682.00
P25–26	537.00	537.00	537.00	**P97**	720.00	720.00	720.00
P27–28	549.00	549.00	549.00	**P98**	718.00	718.00	718.00
P29	501.00	501.00	501.00	**P99**	720.00	720.00	720.00
P30	499.00	499.00	499.00	**P100**	964.00	964.00	964.00
P31–P34	506.00	506.00	506.00	**P101**	958.00	958.00	958.00
P35–P36	500.00	500.00	500.00	**P102**	947.90	947.90	947.90
P37–P38	241.00	241.00	241.00	**P103**	934.00	934.00	934.00
P39	774.00	774.00	774.00	**P104**	935.00	935.00	935.00
P40	769.00	769.00	769.00	**P105**	876.50	876.50	876.50
P41–P42	3.00	3.00	3.00	**P106**	880.90	880.90	880.90
P43–P50	250.00	250.00	250.00	**P107**	873.70	873.70	873.70
P51–54	165.00	165.00	165.00	**P108**	877.40	877.40	877.40
P55–P56	180.00	180.00	180.00	**P109**	871.70	871.70	871.70
P57	103.00	103.00	103.00	**P110**	864.80	864.80	864.80
P58	198.00	198.00	198.00	**P111**	882.00	882.00	882.00
P59	312.00	312.00	312.00	**P112–P114**	94.00	94.00	94.00
P60	308.60	308.59	308.59	**P115–P117**	244.00	244.00	244.00
P61	163.00	163.00	163.00	**P118–P119**	95.00	95.00	95.00
P62	95.00	95.00	95.00	**P120**	116.00	116.00	116.00
P63	511.00	503.05	503.05	**P121**	175.00	175.00	175.00
P64	511.00	511.00	511.00	**P122**	2.00	2.00	2.00
P65	490.00	490.00	490.00	**P123**	4.00	4.00	4.00
P66	256.84	256.80	256.80	**P124**	15.00	15.00	15.00
P67–P68	490.00	490.00	490.00	**P125**	9.00	9.00	9.00
P69	130.00	130.00	130.00	**P126**	12.00	12.00	12.00
P70	294.56	294.58	294.58	**P127**	10.00	10.00	10.00
P71	141.59	141.67	141.67	**P128**	112.00	112.00	112.00
P72	365.92	365.95	365.95	**P129**	4.00	4.00	4.00
P73	195.00	195.00	195.00	**P130–P131**	5.00	5.00	5.00
P74	217.10	204.67	204.67	**P132**	50.00	50.00	50.00
P75	217.89	241.27	241.27	**P133**	5.00	5.00	5.00
P76	258.68	257.86	257.86	**P134–P135**	42.00	42.00	42.00
P77	403.29	400.96	400.96	**P136**	41.00	41.00	41.00

Table A5. *Cont.*

Units	QOGWO	IGWO	GWO	Units	QOGWO	IGWO	GWO
P78	330.00	330.00	330.00	**P137**	17.00	17.00	17.00
P79–80	531.00	531.00	531.00	**P138–P139**	7.00	7.00	7.00
P81	542.00	542.00	542.00	**P140**	26.00	26.00	26.00
Fcost (USD/h)					1,655,679.43	1,655,679.57	1,655,685.80

Table A6. Optimal generation schedule for test system III-B.

Units	QOGWO	IGWO	GWO	Units	QOGWO	IGWO	GWO
P1	119.00	119.00	119.00	**P82**	56.00	56.00	56.00
P2	164.00	164.00	164.00	**P83–P84**	115.00	115.00	115.00
P3–P4	190.00	190.00	190.00	**P86–P87**	207.00	207.00	207.00
P5	168.54	168.54	168.54	**P88–P89**	175.00	175.00	175.00
P6	190.00	190.00	190.00	**P90**	180.41	180.42	180.62
P7–P8	490.00	490.00	490.00	**P91**	175.00	175.00	175.00
P9–P12	496.00	496.00	496.00	**P92**	575.40	575.40	575.40
P13	506.00	506.00	506.00	**P93**	547.50	547.50	547.50
P14	509.00	509.00	509.00	**P94**	836.80	836.80	836.80
P15	506.00	506.00	506.00	**P95**	837.50	837.50	837.50
P16	505.00	505.00	505.00	**P96**	682.00	682.00	682.00
P17–P18	506.00	506.00	506.00	**P97**	720.00	720.00	720.00
P19–P24	505.00	505.00	505.00	**P98**	718.00	718.00	718.00
P25–P26	537.00	537.00	537.00	**P99**	720.00	720.00	720.00
P27–P28	549.00	549.00	549.00	**P100**	964.00	964.00	964.00
P29	501.00	501.00	501.00	**P101**	958.00	958.00	958.00
P30	499.00	499.00	499.00	**P102**	947.90	947.90	947.90
P31–P34	506.00	506.00	506.00	**P103**	934.00	934.00	934.00
P35–P36	500.00	500.00	500.00	**P104**	935.00	935.00	935.00
P37–P38	241.00	241.00	241.00	**P105**	876.50	876.50	876.50
P39	774.00	774.00	774.00	**P106**	880.90	880.90	880.90
P40	769.00	769.00	769.00	**P107**	873.70	873.70	873.70
P41–P42	3.00	3.00	3.00	**P108**	877.40	877.40	877.40
P43–P50	250.00	250.00	250.00	**P109**	871.70	871.70	871.70
P51–P54	165.00	165.00	165.00	**P110**	864.80	864.80	864.80
P55–P56	180.00	180.00	180.00	**P111**	882.00	882.00	882.00
P57	103.00	103.00	103.00	**P112–P114**	94.00	94.00	94.00
P58	198.00	198.00	198.00	**P115–P117**	244.00	244.00	244.00
P59	312.00	312.00	312.00	**P118–P119**	95.00	95.00	95.00
P60	308.59	308.59	308.73	**P120**	116.00	116.00	116.00
P61	163.00	163.00	163.00	**P121**	175.00	175.00	175.00
P62	95.00	95.00	95.00	**P122**	2.00	2.00	2.00
P63–P64	511.00	511.00	511.00	**P123**	4.00	4.00	4.00

Table A6. *Cont.*

Units	QOGWO	IGWO	GWO	Units	QOGWO	IGWO	GWO
P65	490.00	490.00	490.00	**P124**	15.00	15.00	15.00
P66	256.75	256.81	257.47	**P125**	9.00	9.00	9.00
P67–P68	490.00	490.00	490.00	**P126**	12.00	12.00	12.00
P69	130.00	130.00	130.00	**P127**	10.00	10.00	10.00
P70	339.44	339.44	339.44	**P128**	112.00	112.00	112.00
P71	141.59	141.59	141.82	**P129**	4.00	4.00	4.00
P72	388.33	388.33	388.33	**P130–P131**	5.00	5.00	5.00
P73	195.00	195.00	195.00	**P132**	50.00	50.00	50.00
P74	196.23	214.74	195.10	**P133**	5.00	5.00	5.00
P75	196.10	175.00	175.00	**P134–P135**	42.00	42.00	42.00
P76	257.97	258.57	262.69	**P136**	41.00	41.00	41.00
P77	400.95	402.89	417.18	**P137**	17.00	17.00	17.00
P78	330.00	330.00	330.00	**P138–P139**	7.00	7.00	7.00
P79–P80	531.00	531.00	531.00	**P140**	26.00	26.00	26.00
P81	542.00	542.00	542.00	**Fcost (USD/h)**	1,657,962.73	1,657,962.76	1,657,962.89

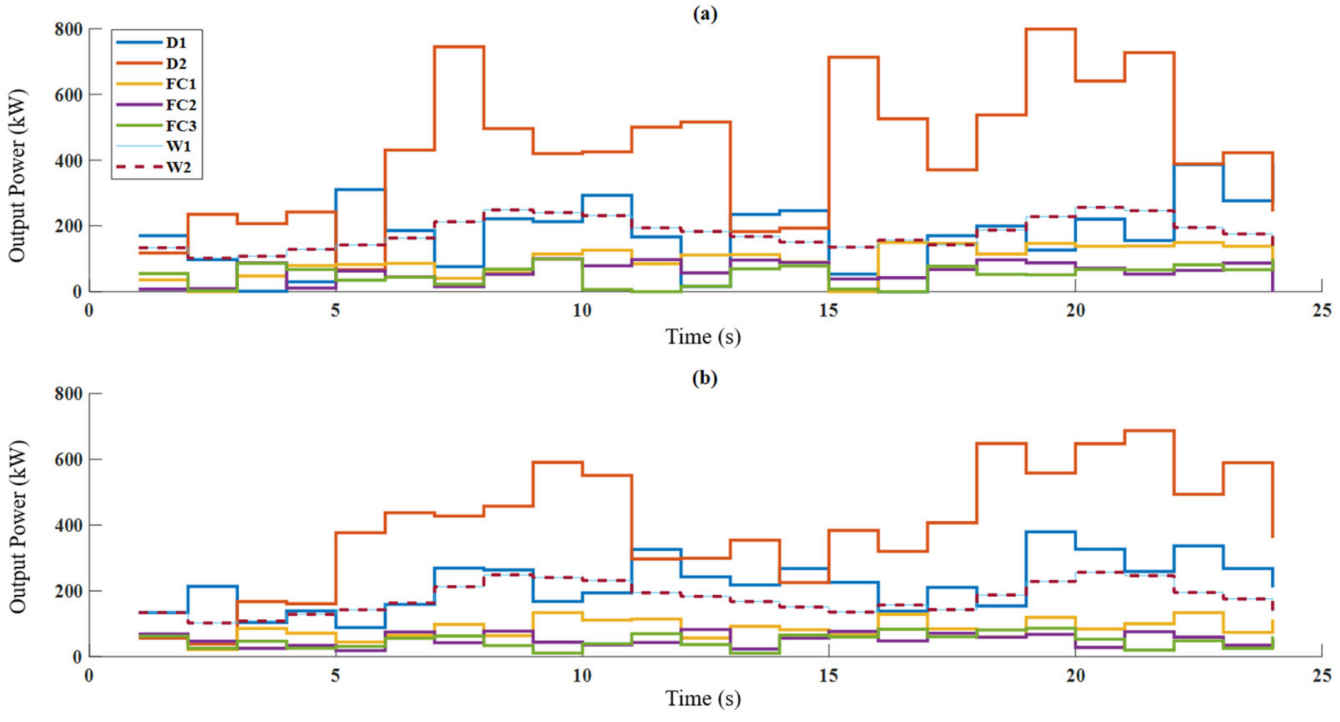

Figure A1. Optimal generation for test system IV obtained using (**a**) GWO and (**b**) IGWO.

Table A7. Optimal generation schedule for test system IV obtained using mQOGWO.

D1 (kW)	D2 (kW)	FC1 (kW)	FC2 (kW)	FC3 (kW)	W1 (kW)	W2 (kW)
134.76	83.08	72.96	55.29	40.87	133.52	133.52
81.21	105.20	54.34	47.58	57.03	102.32	102.32
101.16	153.55	82.55	45.61	46.40	107.87	107.87
119.89	152.48	72.88	35.49	49.74	128.76	128.76
157.25	248.01	57.25	46.59	49.20	142.35	142.35
183.20	408.02	88.68	47.62	64.13	163.17	163.17
285.25	405.09	89.80	52.50	67.15	212.61	212.61
241.02	451.45	89.76	68.34	45.75	248.84	248.84
248.55	519.03	80.72	55.62	42.84	240.62	240.62
244.58	452.48	109.14	66.71	57.25	231.42	231.42
200.82	473.70	74.38	56.16	44.68	194.13	194.13
216.78	315.30	80.32	56.78	48.31	183.26	183.26
229.70	312.38	62.48	42.34	50.21	167.45	167.45
169.26	363.63	68.49	38.10	57.06	150.73	150.73
249.75	393.50	77.99	42.64	49.32	135.41	135.41
210.96	328.56	68.45	56.19	53.62	157.11	157.11
234.01	404.81	80.35	54.71	58.82	142.66	142.66
251.32	545.20	90.02	55.13	59.57	187.38	187.38
329.19	672.45	103.10	56.86	49.57	228.42	228.42
296.41	640.66	95.03	55.11	51.63	256.58	256.58
264.04	645.94	91.95	74.59	65.01	246.24	246.24
355.50	517.98	89.65	53.49	54.89	195.25	195.25
268.85	461.29	141.94	65.76	53.27	175.44	175.44
222.58	370.71	90.00	56.34	55.16	135.61	135.61

References

1. Boussaïd, I.; Lepagnot, J.; Siarry, P. A survey on optimization metaheuristics. *Inf. Sci.* **2013**, *237*, 82–117. [CrossRef]
2. Ezugwu, A.E.; Shukla, A.K.; Nath, R.; Akinyelu, A.A.; Agushaka, J.O.; Chiroma, H.; Muhuri, P.K. Nath Metaheuristics: A comprehensive overview and classification along with bibliometric analysis. *Artif. Intell. Rev.* **2021**, *54*, 4237–4316. [CrossRef]
3. Mirjalili, S.; Dong, J.S.; Sadiq, A.S.; Faris, H. Genetic Algorithm: Theory, Literature Review, and Application in Image Reconstruction. In *Nature-Inspired Optimizers, Studies in Computational Intelligence*; Mirjalili, S., Song Dong, J., Lewis, A., Eds.; Springer: Cham, Switzerland, 2020; Volume 811. [CrossRef]
4. Das, S.; Suganthan, P.N. Differential evolution: A survey of the state-of-the-art. *IEEE Trans. Evol. Comput.* **2011**, *15*, 4–31. [CrossRef]
5. Neto, R.F.T.; Filho, M.G. Literature review regarding Ant Colony Optimization applied to scheduling problems: Guidelines for implementation and directions for future research. *Eng. Appl. Artif. Intell.* **2013**, *26*, 150–161. [CrossRef]
6. Banks, A.; Vincent, J.; Anyakoha, C. A review of particle swarm optimization. Part I: Background and development. *Nat. Comput.* **2007**, *6*, 467–484. [CrossRef]
7. Banks, A.; Vincent, J.; Anyakoha, C. A review of particle swarm optimization. Part II: Hybridization, combinatorial, multicriteria and constrained optimization, and indicative applications. *Nat. Comput.* **2008**, *7*, 109–124. [CrossRef]
8. Karaboga, D.; Gorkemli, B.; Ozturk, C.; Karaboga, N. A comprehensive survey: Artificial bee colony (ABC) algorithm and applications. *Artif. Intell. Rev.* **2014**, *42*, 21–57. [CrossRef]
9. Fister, I.; Fister, I., Jr.; Yang, X.-S.; Brest, J. A comprehensive review of firefly algorithms. *Swarm Evol. Comput.* **2013**, *13*, 34–46. [CrossRef]
10. Bolaji, A.L.; Al-Betar, M.A.; Awadallah, M.A.; Khader, A.T.; Abualigah, L.M. A comprehensive review: Krill Herd algorithm (KH) and its applications. *Appl. Soft Comput.* **2016**, *49*, 437–446. [CrossRef]

11. Rani, B.S.; Kumar, C.A. A comprehensive review on bacteria foraging optimization technique. In *Multi-Objective Swarm Intelligence*; Springer: Berlin/Heidelberg, Germany, 2015; pp. 1–25.
12. Rana, N.; Latiff, M.S.A.; Abdulhamid, S.M.; Misra, S. A hybrid whale optimization algorithm with differential evolution optimization for multiobjective virtual machine scheduling in cloud computing. *Eng. Optim.* **2021**, *53*, 1–18. [CrossRef]
13. Mirjalili, S.; Mirjalili, S.M.; Lewis, A. Grey wolf optimizer. *Adv. Eng. Softw.* **2014**, *69*, 46–61. [CrossRef]
14. Ma, H.; Simon, D.; Siarry, P.; Yang, Z.; Fei, M. Biogeography-based optimization: A 10-year review. *IEEE Trans. Emerg. Top. Comput. Intell.* **2017**, *1*, 391–407. [CrossRef]
15. Yang, X.S.; He, X. Bat algorithm: Literature review and applications. *Int. J. Bio-Inspired Comput.* **2013**, *5*, 141–149. [CrossRef]
16. Abdel-Basset, M.; Shawky, L.A. Flower pollination algorithm: A comprehensive review. *Artif. Intell. Rev.* **2019**, *52*, 2533–2557. [CrossRef]
17. Suman, B.; Kumar, P. A survey of simulated annealing as a tool for single and multiobjective optimization. *J. Oper. Res. Soc.* **2006**, *57*, 1143–1160. [CrossRef]
18. Rashedi, E.; Rashedi, E.; Nezamabadi-pour, H. A comprehensive survey on gravitational search algorithm. *Swarm Evol. Comput.* **2018**, *41*, 141–158. [CrossRef]
19. Zou, F.; Chen, D.; Xu, Q. A survey of teaching–learning-based optimization. *Neurocomputing* **2019**, *335*, 366–383. [CrossRef]
20. Xue, R.; Wu, Z. A survey of application and classification on teaching-learning-based optimization algorithm. *IEEE Access* **2020**, *8*, 1062–1079. [CrossRef]
21. Nayak, S.C.; Misra, B.B. A chemical-reaction-optimization-based neuro-fuzzy hybrid network for stock closing price prediction. *Financ. Innov.* **2019**, *5*, 38. [CrossRef]
22. Hatta, N.M.; Zain, A.M.; Sallehuddin, R.; Shayfull, Z.; Yusoff, Y. Recent studies on optimisation method of Grey Wolf Optimiser (GWO): A review (2014–2017). *Artif. Intell. Rev.* **2019**, *52*, 2651–2683. [CrossRef]
23. Pradhan, M.; Roy, P.K.; Pal, T. Grey wolf optimization applied to economic load dispatch problems. *Int. J. Electr. Power Energy Syst.* **2016**, *83*, 325–334. [CrossRef]
24. Sharma, K.; Dubey, H.M.; Pandit, M. Short-term hydrothermal scheduling using gray wolf optimization. In *Advances in Computing and Intelligent Systems*; Pandit, M., Dubey, H.M., Bansal, J.C., Eds.; Springer: Singapore, 2020; pp. 253–269. [CrossRef]
25. Jayakumar, N.; Subramanian, S.; Ganesan, S.; Elanchezhian, E.B. Grey wolf optimization for combined heat and power dispatch with cogeneration systems. *Int. J. Electr. Power Energy Syst.* **2016**, *74*, 252–264. [CrossRef]
26. Nimma, K.; Al-Falahi, M.; Nguyen, H.D.; Jayasinghe, S.D.G.; Mahmoud, T.; Negnevitsky, M. Grey wolf optimization-based optimum energy-management and battery-sizing method for grid-connected microgrids. *Energies* **2018**, *11*, 847. [CrossRef]
27. Sultana, U.; Khairuddin, A.B.; Mokhtar, A.S.; Zareen, N.; Sultana, B. Grey wolf optimizer based placement and sizing of multiple distributed generation in the distribution system. *Energy* **2016**, *111*, 525–536. [CrossRef]
28. Verma, S.K.; Yadav, S.; Nagar, S.K. Optimization of fractional order PID controller using grey wolf optimizer. *J. Control. Autom. Electr. Syst.* **2017**, *28*, 314–322. [CrossRef]
29. Li, S.-X.; Wang, J.-S. Dynamic modeling of steam condenser and design of PI controller based on grey wolf optimizer. *Math. Probl. Eng.* **2015**, *2015*, 120975. [CrossRef]
30. Precup, R.-E.; David, R.-C.; Petriu, E.M. Grey wolf optimizer algorithm-based tuning of fuzzy control systems with reduced parametric sensitivity. *IEEE Trans. Ind. Electron.* **2017**, *64*, 527–534. [CrossRef]
31. Zin, T.T.; Lin, J.C.-W.; Pan, J.-S.; Tin, P.; Yokota, M. (Eds.) Genetic and evolutionary computing. In Proceedings of the Ninth International Conference on Genetic and Evolutionary Computing, Yangon, Myanmar, 26–28 August 2015; Springer International Publishing: Cham, Switzerland, 2016; Volume 1.
32. Fouad, M.M.; Hafez, A.I.; Hassanien, A.E.; Snasel, V. Grey Wolves Optimizer-based localization approach in WSNs. In Proceedings of the 2015 11th International Computer Engineering Conference (ICENCO), Cairo, Egypt, 29–30 December 2015; pp. 256–260.
33. Zhang, S.; Zhou, Y. Template matching using grey wolf optimizer with lateral inhibition. *Optik* **2017**, *130*, 1229–1243. [CrossRef]
34. Chowdhury, A.A.; Borkar, V.S.; Birajdar, G.K. Indian language identification using time-frequency image textural descriptors and GWO-based feature selection. *J. Exp. Theor. Artif. Intell.* **2020**, *32*, 111–132. [CrossRef]
35. Gupta, E.; Saxena, A. Grey wolf optimizer-based regulator design for automatic generation control of interconnected power system. *Cogent Eng.* **2016**, *3*, 1151612. [CrossRef]
36. Song, X.; Tang, L.; Zhao, S.; Zhang, X.; Li, L.; Huang, J.; Cai, W. Grey Wolf Optimizer for parameter estimation in surface waves. *Soil Dyn. Earthq. Eng.* **2015**, *75*, 147–157. [CrossRef]
37. Luo, Q.; Zhang, S.; Li, Z.; Zhou, Y. A novel complex-valued encoding grey wolf optimization algorithm. *Algorithms* **2015**, *9*, 4. [CrossRef]
38. Zhang, S.; Zhou, Y. Grey wolf optimizer based on Powell local optimization method for clustering analysis. *Discret. Dyn. Nat. Soc.* **2015**, *2015*, 481360. [CrossRef]
39. Jayabarathi, T.; Raghunathan, T.; Adarsh, B.R.; Suganthan, P.N. Economic dispatch using hybrid grey wolf optimizer. *Energy* **2016**, *111*, 630–641. [CrossRef]
40. Mittal, N.; Singh, U.; Sohi, B.S. Modified Grey Wolf Optimizer for global engineering optimization. *Appl. Comput. Intell. Soft Comput.* **2016**, *2016*, 7950348. [CrossRef]
41. Oliveira, J.; Oliveira, P.M.; Boaventura-Cunha, J.; Pinho, T. Chaos-based grey wolf optimizer for higher order sliding mode position control of a robotic manipulator. *Nonlinear Dyn.* **2017**, *90*, 1353–1362. [CrossRef]

42. Singh, N.; Singh, S.B. A modified mean gray wolf optimization approach for benchmark and biomedical problems. *Evol. Bioinform.* **2017**, *13*, 1176934317729413. [CrossRef] [PubMed]
43. Singh, D.; Dhillon, J.S. Ameliorated grey wolf optimization for economic load dispatch problem. *Energy* **2019**, *169*, 398–419. [CrossRef]
44. Pradhan, M.; Roy, P.K.; Pal, T. Oppositional based grey wolf optimization algorithm for economic dispatch problem of power system. *Ain Shams Eng. J.* **2018**, *9*, 2015–2025. [CrossRef]
45. Long, W.; Jiao, J.; Liang, X.; Tang, M. Inspired grey wolf optimizer for solving large-scale function optimization problems. *Appl. Math. Model.* **2018**, *60*, 112–126. [CrossRef]
46. Al-Tashi, Q.; Kadir, S.J.A.; Rais, H.M.; Mirjalili, S.; Alhussian, H. Binary optimization using hybrid grey wolf optimization for feature selection. *IEEE Access* **2019**, *7*, 39496–39508. [CrossRef]
47. Al-Betar, M.A.; Awadallah, M.A.; Krishan, M.M. A nonconvex economic load dispatch problem with valve loading effect using a hybrid grey wolf optimizer. *Neural Comput. Appl.* **2020**, *32*, 12127–12154. [CrossRef]
48. Nanda, S.J.; Sharma, M.; Panda, A. Clustering big datasets using orthogonal gray wolf optimizer. In Proceedings of the 2019 International Conference on Information Technology (ICIT), Guangzhou, China, 20–22 December 2019; pp. 353–358.
49. Gupta, S.; Deep, K.; Mirjalili, S. Accelerated grey wolf optimiser for continuous optimisation problems. *Int. J. Swarm Intell.* **2020**, *5*, 22–59. [CrossRef]
50. Yan, F.; Xu, X.; Xu, J. Grey wolf optimizer with a novel weighted distance for global optimization. *IEEE Access* **2020**, *8*, 120173–120197. [CrossRef]
51. Das, D.; Bhattacharya, A.; Ray, R.N. Quasi-oppositional grey wolf optimizer algorithm for economic dispatch. *Indian J. Sci. Technol.* **2018**, *11*, 41.
52. Saxena, A.; Soni, B.P.; Kumar, R.; Gupta, V. Intelligent Grey Wolf Optimizer–Development and application for strategic bidding in uniform price spot energy market. *Appl. Soft Comput.* **2018**, *69*, 1–13. [CrossRef]
53. Basu, M.; Chowdhury, A. Cuckoo search algorithm for economic dispatch. *Energy* **2013**, *60*, 99–108. [CrossRef]
54. Wais, P. A review of Weibull functions in wind sector. *Renew. Sustain. Energy Rev.* **2017**, *70*, 1099–1107. [CrossRef]
55. Mahdavi, S.; Rahnamayan, S.; Deb, K. Opposition based learning: A literature review. *Swarm Evol. Comput.* **2018**, *39*, 1–23. [CrossRef]
56. Xu, Q.; Guo, L.; Wang, N.; He, Y. COOBBO: A novel opposition-based soft computing algorithm for TSP problems. *Algorithms* **2014**, *7*, 663–684. [CrossRef]
57. Mandal, B.; Roy, P.K. Optimal reactive power dispatch using quasi-oppositional teaching learning-based optimization. *Int. J. Electr. Power Energy Syst.* **2013**, *53*, 123–134. [CrossRef]
58. Suid, M.H.; Ahmad, M.A.; Ismail, M.R.T.R.; Ghazali, M.R.; Irawan, A.; Tumari, M.Z. An improved sine cosine algorithm for solving optimization problems. In Proceedings of the 2018 IEEE Conference on Systems, Process and Control (ICSPC), Melaka, Malaysia, 14–15 December 2018.
59. Hussain, K.; Salleh, M.N.M.; Cheng, S.; Naseem, R. Common benchmark functions for metaheuristic evaluation: A review. *JOIV Int. J. Inform. Vis.* **2017**, *1*, 218–223. [CrossRef]
60. Jamil, M.; Yang, X.S. A literature survey of benchmark functions for global optimisation problems. *Int. J. Math. Model. Numer. Optim.* **2013**, *4*, 150. [CrossRef]
61. Ciornei, I.; Kyriakides, E. A GA-API solution for the economic dispatch of generation in power system operation. *IEEE Trans. Power Syst.* **2012**, *27*, 233–242. [CrossRef]
62. Park, J.B.; Jeong, Y.W.; Shin, J.R.; Lee, K.Y. An improved particle swarm optimization for nonconvex economic dispatch problems. *IEEE Trans. Power Syst.* **2010**, *25*, 156–166. [CrossRef]
63. Panigrahi, B.K.; Yadav, S.R.; Agrawal, S.; Tiwari, M.K. A clonal algorithm to solve economic load dispatch. *Electr. Power Syst. Res.* **2007**, *77*, 1381–1389. [CrossRef]
64. Pothiya, S.; Ngamroo, I.; Kongprawechnon, W. Application of multiple tabu search algorithm to solve dynamic economic dispatch considering generator constraints. *Energy Convers. Manag.* **2008**, *49*, 506–516. [CrossRef]
65. Khamsawang, S.; Jiriwibhakorn, S. DSPSO–TSA for economic dispatch problem with non-smooth and noncontinuous cost functions. *Energy Convers. Manag.* **2010**, *51*, 365–375. [CrossRef]
66. Yu, J.-T.; Kim, C.-H.; Wadood, A.; Khurshaid, T.; Rhee, S.-B. Jaya algorithm with self-adaptive multi-population and Lévy flights for solving economic load dispatch problems. *IEEE Access* **2019**, *7*, 21372–21384. [CrossRef]
67. Yu, J.; Kim, C.-H.; Wadood, A.; Khurshiad, T.; Rhee, S.-B. A novel multi-population based chaotic JAYA algorithm with application in solving economic load dispatch problems. *Energies* **2018**, *11*, 1946. [CrossRef]
68. Bhattacharjee, K.; Bhattacharya, A.; Dey, S.H.N. Oppositional Real Coded Chemical Reaction Optimization for different economic dispatch problems. *Int. J. Electr. Power Energy Syst.* **2014**, *55*, 378–391. [CrossRef]
69. Patel, N.; Bhattacharjee, K. A comparative study of economic load dispatch using sine cosine algorithm. *Sci. Iran.* **2020**, *27*, 1467–1480.
70. Barisal, A.K.; Prusty, R.C. Large scale economic dispatch of power systems using oppositional invasive weed optimization. *Appl. Soft Comput.* **2015**, *29*, 122–137. [CrossRef]
71. Pandit, M.; Srivastava, L.; Sharma, M.; Dubey, H.M.; Panigrahi, B.K. Large-scale multi-zone optimal power dispatch using hybrid hierarchical evolution technique. *J. Eng.* **2014**, *2014*, 71–80. [CrossRef]

72. Moradi-Dalvand, M.; Mohammadi-Ivatloo, B.; Najafi, A.; Rabiee, A. Continuous quick group search optimizer for solving nonconvex economic dispatch problems. *Electr. Power Syst. Res.* **2012**, *93*, 93–105. [CrossRef]
73. Dubey, H.M.; Pandit, M.; Panigrahi, B.K. A biologically inspired modified flower pollination algorithm for solving economic dispatch problems in modern power systems. *Cogn. Comput.* **2015**, *7*, 594–608. [CrossRef]
74. Omran, M.G.H.; Clearc, M.; Ghaddar, F.; Aldabagh, A.; Tawfik, O. Permutation Tests for Metaheuristic Algorithms. *Mathematics* **2022**, *10*, 2219. [CrossRef]